Preprints (www.preprints.org) | NOT PEER-REVIEWED | Posted: 18 December 2018 doi:10.20944/preprints201812.0213.v1

EARTHQUAKE TRIGGERED MULTI-HAZARD AND RISK STUDY BASED ON REMOTE SENSING AND GEOGRAPHIC INFORMATION SYSTEM

[1]Aditya Saputra, [2]Christopher Gomez, [3]Ioannis Delikostidis, [3]Peyman Zawar-Reza, [4] Danang Sri Hadmoko, [5]Junun Sartohadi

[1]Fakultas Geografi, Universitas Muhammadiyah Surakarta, Indonesia; [2] Graduate School of Maritime Sciences, Laboratory of Volcanic Risks at Sea Kobe University, 5-1-1 Fukaeminami-machi, Higashinada-ku, Kobe, Japan; [3] Geography Department, University of Canterbury, New Zealand; [4] Geography Faculty, Universitas Gadjah Mada, Yogyakarta, Indonesia; [5] Department of Soil Science, Faculty of Agriculture, Universitas Gadjah Mada, Yogyakarta, Indonesia

Correspondence email: as105@ums.ac.id or aditsaputra1987@gmail.com

ABSTRACT

Yogyakarta City is one of the big city which is located in Java Island, Indonesia. Yogyakarta City, including study area (Pleret Sub District), are very prone to earthquake hazards, because close to several active earthquake sources. For example, Sunda Megathrust which often generates a big earthquake which can affect the study area. The Sunda Megathrust extends from north to south and west to east along the Sumatra and Java Islands. Furthermore, an active normal fault called as Opak Fault pass through right in the middle of Study area and divides the study area into east and west zone. Recently, after the devastating earthquake in 2006, the population of the study area increases significantly. As a result, the housing demand is also increasing. However, due to the absence of earthquake building code in the study area, locals tend to build improper new houses. Furthermore, in some part of the mountainous area in the study area, there are some building found in unstable slopes area.

Due to this condition, the multi-hazard and risk study needs to be done in Pleret. The increasing of population and improper houses in Pleret Sub-District can lead to amplify the impact. Thus, the main objective of this study is to assess the multi-hazards and risk of earthquake and other related secondary hazards such as ground amplification, liquefaction, and coseismic landslide. The method mainly utilised the geographic information system, remote sensing and was fit up by the outcrop study.

The results show that the middle part of the study area has a complex geological structure. It was indicated by a lot of unchartered faults was found in the outcrops. Furthermore, the relatively prone areas to earthquake can be determined. In term of the coseismic landslide, the prone area to the coseismic landslide is located in the east part of the study area in the middle slope of Baturagung Escarpment. The highly potential area of liquefaction is dominated in the central part of the study area. In term of building collapsed probability, the result shows that the safest house based on statistical analysis is the residential house with the building attribute of wood structure, roof cast material, distance more than 15 km from the earthquake source, and located above the Nglanggran Formation. Finally, the multi-hazard and risk analysis show that the middle part of the study area is more vulnerable than the other part of Pleret Sub-District.

Keyword: earthquake multi-hazard and risk, coseismic landslide, outcrop study, liquefaction.

1. Introduction

The cascading hazards received relatively minor attention in disaster and risk management. The majority of hazard and disaster risk studies have concentrated on one single hazard in segregation. They often put less attention to the possibility that one incident can cascade to other secondary hazards and relatively ignored the interaction between hazards [1]. The particular area might be exposed by more than one types of hazards. Each hazard can lead to one single disaster with different size of magnitude [2]. Furthermore, one single incident can trigger other secondary hazards and generate worst cascade impact on the element at risk [3]. For instance, the phenomena of disaster chain in Beichuan due to the 2008 Wenchuan earthquake revealed that the multi-hazard and cascading effect should not be underestimated.

Wenchuan earthquake generated a complex disaster chain which leads to massive damage in Beichuan county town. With shallow focal depth for only about 19 km, this earthquake produced a great ground motion (7.9-8.0 Ms) and caused approximately 90% of the buildings were collapsed. Furthermore, a month later after the devastating earthquake, the flash flood from the Tangjiashan Lake washed the ruins of the collapsed buildings. Afterward, the heavy rainfall generated an extensive mudflow which buried up to 3 stories high of the collapsed buildings. At that time Beichuan county town was closed due to a complex multi-hazards and cascading effect that was triggered by the earthquake. The fault deformation generates an earthquake, the earthquake triggered a coseismic landslide, the coseismic landslide dammed the lake, and the interaction of dammed lake with the heavy rainfall caused a massive alluvial flood.

A similar condition occurred in Christchurch New Zealand. In September 2010 to February 2011, Christchurch, the second largest city in New Zealand, experienced by two sequential big earthquakes. The first earthquake (6.3 Ms) killed 185 people who make this disaster into the second deadliest disaster that ever occur in New Zealand. Furthermore, the second earthquake (7.3 Ms) caused significant damage in the central city of Christchurch. Afterward, in March 2014, Christchurch experienced more flooding due to the impact of the Canterbury Earthquake. Some researchers concluded that this extraordinary flood is not just because of the heavy and prolonged rainfall but, because of ground deformation, liquefaction, subsidence, narrowing of channels and uplifting of river beds after the earthquake [4].

Situated approximately 300 km north of the Java Megathrust Indonesia, the study area (the west flank of Baturagung Escarpment) is very prone to earthquake. Having a total subduction segment of 840 km, the Java Megathrust can potentially generate the earthquake with the maximum magnitude of 8.1 Mw (Fig. 1) [5], which can influence the study area. Additionally, one of an active fault in Java, Opak Fault, passes over this area along the west flank of Baturagung Escarpment. According to [6], with the total length of fault approximately 45 km and slip rate about 2.4 mm per year, Opak fault can also potentially generate shallow earthquake with the maximum magnitude of 6.2 Mw, that can cause a massive destruction to study area and southeast part of Yogyakarta City.

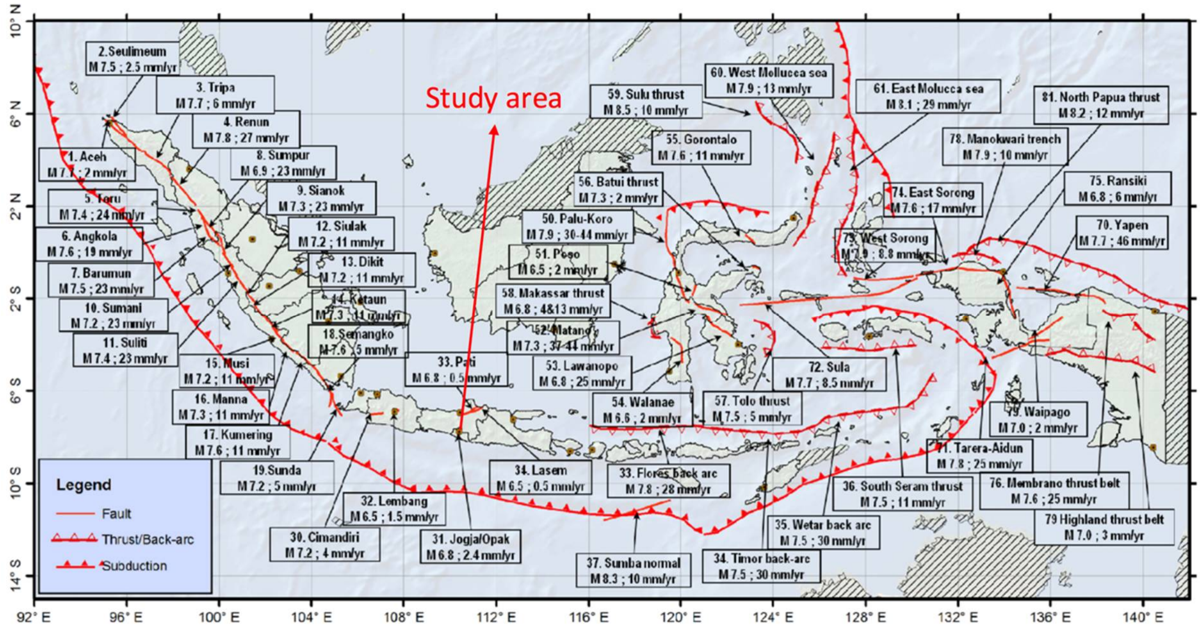

Fig. 1. The segmentation model of subduction earthquake source (Megathrust) in Indonesia, source: [5]

Administratively, the west flank of Baturagung consists of several sub-districts such as Kretek, Pundong, Imogiri, Dlingo, Pleret, and Piyungan. However, due to the complexity of physical characteristics, this study was conducted in Pleret Sub-District, Bantul Regency, Yogyakarta Province, Indonesia. Pleret Sub-District is located approximately 10 km southeast part of Yogyakarta Central City. Located near to subduction zone and passes over by an active Opak Fault make this area is very prone to earthquake hazard. Moreover, the study area is located between the eastern part of Bantul Graben and western flank of Baturagung escarpment which is also prone to coseismic landslide, flood, and liquefaction hazards. High seismicity, prone to ground amplification, the unstable slope in the western flank of Baturagung Escarpment, and liquefaction in the center lowland are the main reason why this study is important to be conducted in the study area.

Probabilistic Seismic Hazard Analysis (PSHA), Deterministic Seismic Hazard Analysis (DSHA), liquefaction, ground motion, landslide and tsunami studies have been well developed in Indonesia.

However, the fact that earthquake can trigger other related hazards cannot be denied. Additionally, the study of multi-hazard and risk in this area is still limited. Thus, the study about earthquake trigger other related secondary hazards are needed in Pleret Sub-District, Southeast part of Yogyakarta Province.

The primary objective of this study is to construct the multi-hazard risk assessment in Pleret Sub-District (Southeast part of Yogyakarta Province) by utilizing the remote sensing and geographic information system. The primary objective can be derived into several series of sub-studies with the objective of; 1) To identify the potential area of coseismic landslide, 2) to conduct the outcrop study in order to get better understanding of fault configuration, 3) to identify the liquefaction zonation, 4) to assess the vulnerability level of some element at risks, and 5) to generate multi-hazard and risk in the study area.

2. Overview of study area

Pleret Sub-District is located 10 km southeast part of Yogyakarta City, Indonesia. In general, the study area is the part of Bantul Graben. This graben formed by two convergent normal faults, which generated two horst zones in the east and the west part and graben zone in the middle part. Two normal faults namely Progo and Opak Faults existed and formed the Bantul Graben. Based on the difference value of gravity, Progo fault can be located near the Progo River in the west, and Opak Fault is located in the border area of Southern Mountain (Baturagung Escarpment) to the east [7]. The study area is located in the transition zone between flat area and the escarpment zone in the eastern part of Bantul Graben (Fig. 2). [8] stated that Pleret Sub-District is located in the eastern Horts of Bantul Graben which was experienced by step faults due to the complexity of specific geological structure.

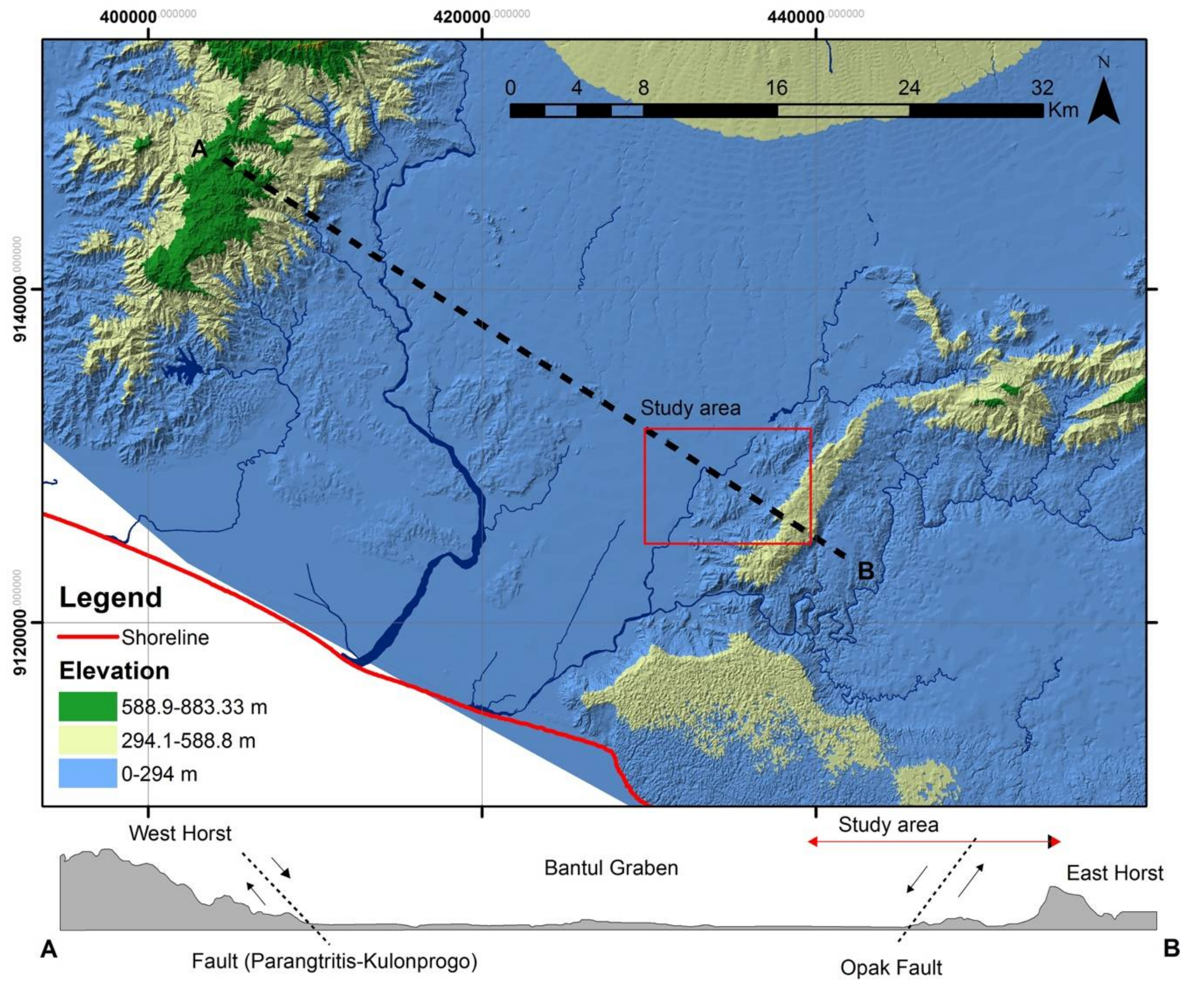

Fig 2. The location of study area which associates with East horst of Bantul Graben.

Physiographically, the study area can be divided into three major zones such as east, middle, and west zones. The west and the middle part zones are dominated by the extensive flat area, while the east zone is dominated by the undulating and mountainous areas. The extensive flat area mainly consists of Young Volcanic Deposits of Merapi Volcano (Qmi) and few of them consist of alluvium (from the denudational process in the eastern mountainous areas) which is located in the foot slope, near the undulating areas. The east part is dominated by the undulating and mountainous area which consists of mainly tertiary deposits of Semilir Formation (Tmse). Meanwhile, only a few of them, including the summit of the Baturagung Escarpment belongs to Nglanggran Formation (Tmn). Tmse formed approximately 27.82-23.03 million years ago. Tmse consists of mainly interbedded layers of breccia pumice, tuff-breccia, dacite tuff, andesite tuff, and tuffaceous clay, while the Tmn was deposited in early Miocene approximately between 23.03 to 11.608 million years ago. Tmn was deposited parallel on the top of Tmse. Tmn mainly distributed in the summit of Baturagung Escarpment in the eastern part of the study area. Both of these formations were generated from the eruption of surrounding

Preprints (www.preprints.org) | NOT PEER-REVIEWED | Posted: 18 December 2018 doi:10.20944/preprints201812.0213.v1

ancient volcano [9-11]. Furthermore, [8] found that both Tmse and Tmn can be classified as pyroclastic density flow from the ancient volcano that might be located in the east part of the study area.

In term of geomorphology, three major groups of landforms can be identified in the study area such as structural, fluvial and denudation landforms. The structural landforms can be indicated by the existence of Baturagung Escarpment in the east part. The intensive denudation process also occurred in the middle to upper slope of the escarpment. Some triangle facet also formed due to high erosion process in the middle to upper slope of the escarpment. The other geomorphic process such as fluvial process occurs in the middle part of the study area along the Opak River. Furthermore, the fluvial process also takes place in the narrow flat area near the undulating area and Baturagung Escarpment. The fluvial process along the Opak River and narrow flat area generated extensive alluvial plain and colluvial plain, respectively. The alluvial plain consists of Qmi, while the colluvium consists of Qa (denudation material from Semilir and Nglanggran Formation). Please see Fig. 3 for a better description of the geomorphological aspect.

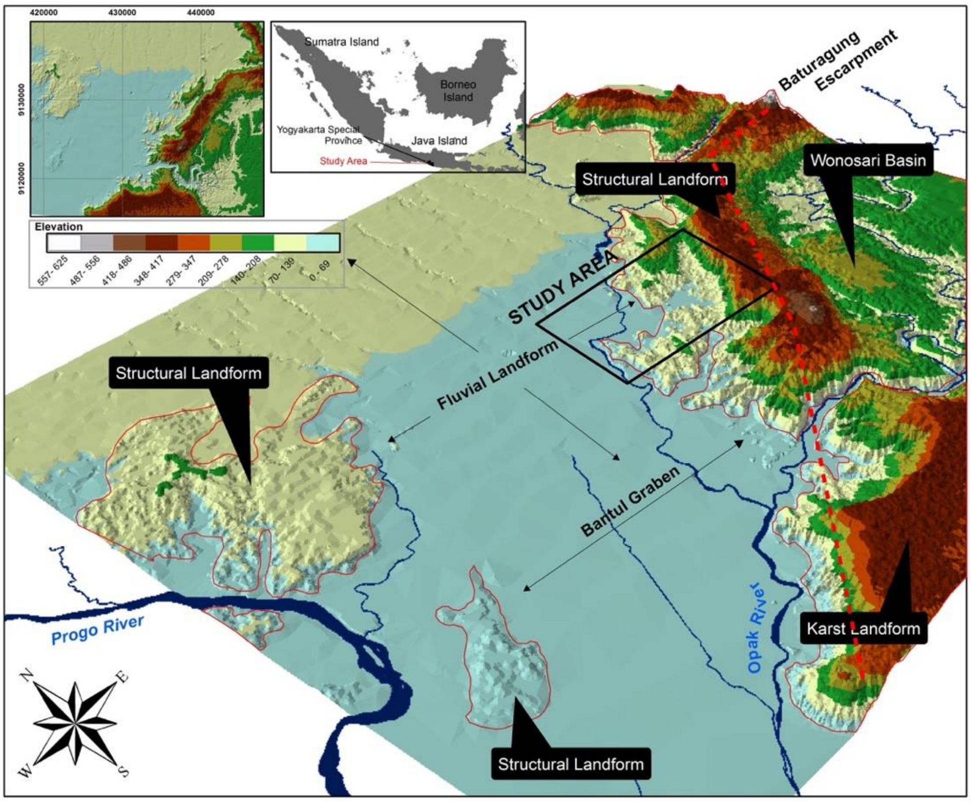

Fig. 3. The general landform of study area and surroundings.

3. Method

3.1. Scope of the analysis

Situated in a complex geological and geomorphological condition, the study area is more prone to several hazards. The study area has high seismic activities due to the location. Pleret Sub-District is

Preprints (www.preprints.org) | NOT PEER-REVIEWED | Posted: 18 December 2018 doi:10.20944/preprints201812.0213.v1

located approximately 250 km north of active Sunda Megathrust and passed by one of the active inland fault namely Opak Fault. The middle part of the study area also prone to soil amplification because this area is dominated by dense quaternary material of Merapi Volcano. Furthermore, the abundance of shallow groundwater in this area can also potentially generate liquefaction. The mountainous area in the east part of the study area is also prone to slope stability and coseismic landslide due to the type of lithology and intensive erosion. Based on this consideration, this multi-risk study only covers earthquake, soil amplification, liquefaction, and coseismic landslide aspects.

3.2. Data

The probabilistic seismic hazard analysis and liquefaction analysis was mainly used the historic earthquake data from USGS between 1973 and 2017. The fieldwork data of outcrop study [8] and seismic vulnerability index (kg) from microtremor measurement [12] were also used in the earthquake and liquefaction analysis, respectively. Additionally, the direct measurement data of groundwater which was obtained from household well measurement, and few of borehole and geo-electric data were used to support the analysis of groundwater condition in the middle part of the study area. The analysis of coseismic landslide used mainly rainfall data from several weather stations surrounding study area, 1: 25,000 topographic map, and detailed geology map which was obtained from remote sensing interpretation and fieldwork observation by [13-14].

In term of vulnerability assessment, the detail land use data and building damage were used in this analysis. The land use data was generated by using the visual interpretation of the latest Quickbird image, 2012 [15]. Meanwhile, the building damage data due to the 2006 Yogyakarta earthquake was obtained from the previous research conducted by [16]. The list of data used in this study is provided in Table 1.

Table 1. The data usage in this study

No	Data	Scale	Format	source	Used for
1	The earthquake data history	- year 1973-2014 - Magnitude greater than 5 Richter - Earthquake surrounding Java	Tabular data .csv format	USGS	To generate PGA in earthquake hazard assessment and liquefaction analysis
2	Predominant frequency of soil	Bantul Regency	Tabular data .xml format	[12]	To generate PGA and support liquefaction analysis
3	Rainfall data	Yogyakarta Province	Tabular data .xml format	Weather stations *	To generate coseismic landslide hazard

 doi:10.20944/preprints201812.0213.v1

4	Geology map of Yogyakarta	1:100,000	Raster .jpg format	Geological Research and Development Centre, Bandung Indonesia	To generate coseismic landslide hazard, outcrop distribution, and support outcrop study
5	Contour map	1:25,000 Contour interval 12.5. m	Vector shapefile format	Indonesian Geospatial information agency	To generate coseismic landslide hazard
6.	Outcrop distribution	1:35,000	Vector shapefile format	Quickbird imagery interpretation	Support outcrop study and earthquake susceptibility based on the proximity of faults.
7	Micro faults and rock-layer characteristics of the outcrop	1:25,000	Vector shapefile format	fieldwork	Support outcrop study and earthquake susceptibility based on the proximity of faults.
8	3d surface of the outcrop	Unit outcrop	Raster, format geo tiff	Structure from motion	Support outcrop study
9	Microtremor data	Regency level	Tabular .xml format	[12]	Liquefaction analysis
10	Groundwater table depth	Sub-district level	Vector shapefile format	- Household well survey - Geo-electric survey - Borehole	Liquefaction analysis
11	Building damage data due to 2006 Yogyakarta earthquake	Provincial level	Vector shapefile format	[16]	Deterministic model of building damage
12	Type of occupation	Sub-district level	Tabular report form	Statistics Indonesia	Population modelling.

3.3. The outcrop study

The outcrop study could be divided into three main stage: first, pre-fieldwork analysis, fieldwork activities, and post-fieldwork analysis. The pre-fieldwork analysis consists of geological data (lithological and geological structure) extraction from mainly Yogyakarta Geology map scale 1:100,000 and Landsat 8 interpretation (please refers to [8]). Additionally, the visual interpretation of Quickbird imagery was also conducted in the pre-fieldwork analysis of the outcrop study. The primary purpose of the interpretation was to identify the location of the outcrop and determine the location of outcrop observation. The fieldwork activities were to characterise the outcrop (identify the lithofacies and qualitative grain size of each rock layer), identify the micro fault, and to record the 3d surface model of the outcrop by using structure from motion technique to support the further outcrop study. The brief workflow of outcrop study stage is provided in Figure 4 below.

Preprints (www.preprints.org) | NOT PEER-REVIEWED | Posted: 18 December 2018 doi:10.20944/preprints201812.0213.v1

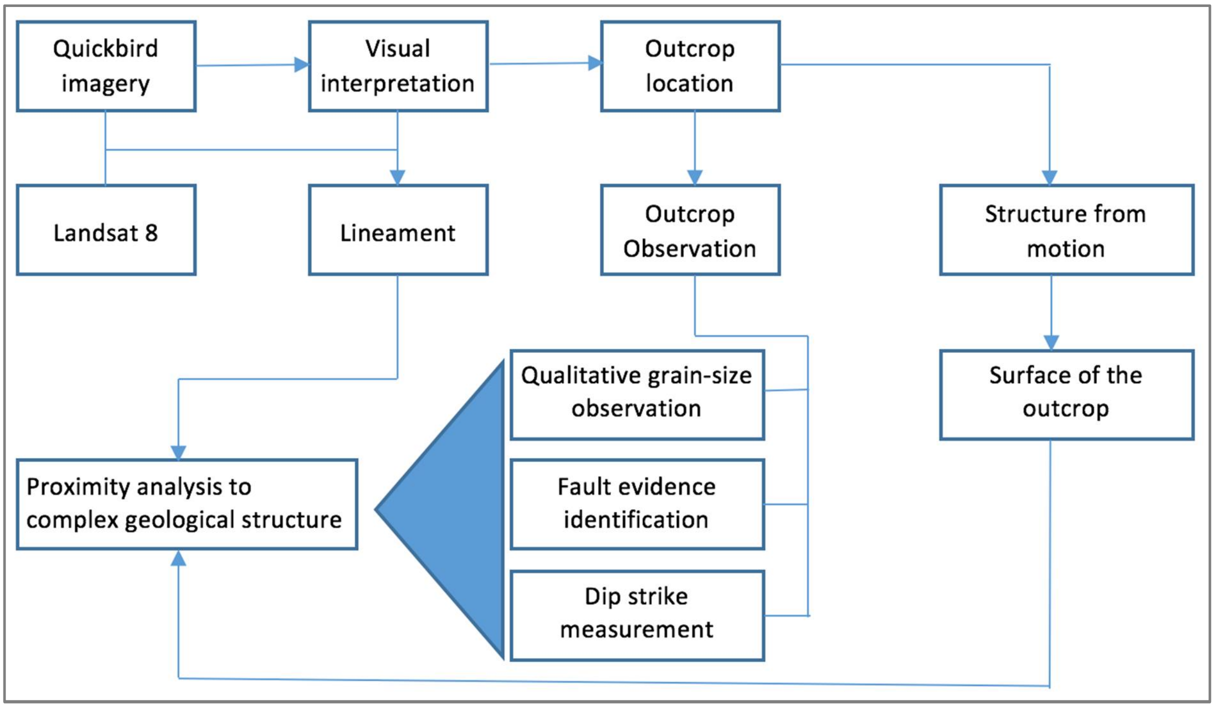

Fig. 4. The general work flow of outcrop study

3.4. The Coseismic landslide assessment

The coseismic landslide susceptibility analysis on this multi-hazard and risk study used the result of previous research conducted by [14]. This study applied method which was proposed by [17]. There were two main parameters such as site characteristic factors and trigger factors that might cause coseismic landslide occurrence. Site characteristics consist of physical parameters which are closed to stability analysis including relief, geology, and soil humidity. Meanwhile, the trigger factors consist of seismic and rainfall intensity.

As stated above in Table 1 the other spatial data such as relief and lithology were derived from contour and geology map, respectively. The contour map resolution is about 12.5 m. Meanwhile, the geology map scale is 1: 100,000. [14] had been conducted some remote sensing interpretation and fieldwork observation to increase the scale of geology map and produced more detailed geology and lithology information. The other parameters such as natural humidity of soil and rainfall intensity were derived from monthly average rainfall and annual rainfall intensity, respectively. The detailed work step of coseismic landslide assessment which was conducted by [14] is provided in Figure 5 below.

Preprints (www.preprints.org) | NOT PEER-REVIEWED | Posted: 18 December 2018 doi:10.20944/preprints201812.0213.v1

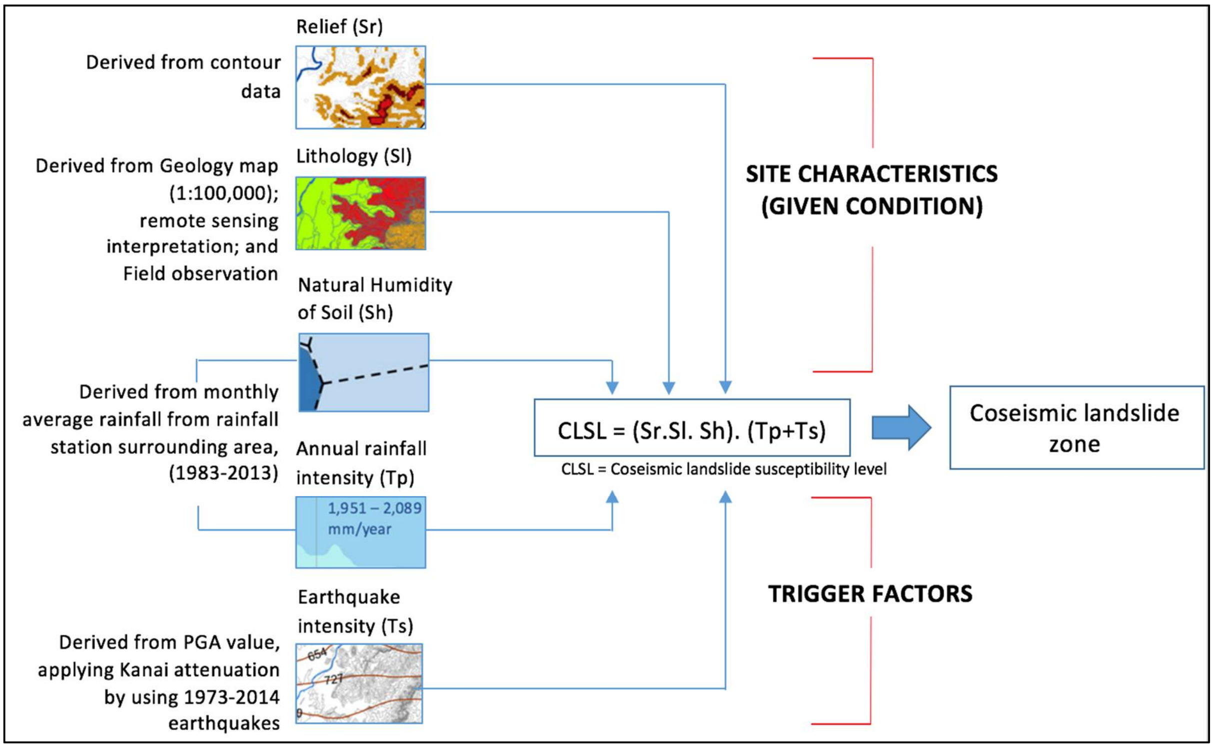

Fig. 5. The general workflow of coseismic landslide susceptibility zone [14].

3.5. The liquefaction assessment

Liquefaction is a secondary earthquake hazard that often causes the worst damage to some big cities around the world. In 1999, 7.6 Mw earthquake occurred in Chi-Chi Taiwan. This earthquake generated massive liquefaction over Taiwan especially in Nantou, Wufeng, and Yuanlin prefecture [18]. In New Zealand, two strong sequential earthquakes in September 2010 and December 2011 in Christchurch caused massive liquefaction across Christchurch [19]. Recently, 28 September 2018, strong earthquake struck Palu City, Central Sulawesi, Indonesia. Palu-Koro strike-slip fault generated inland earthquake with the magnitude of 7.4 Richter scale and earthquake depth of 10 km. This earthquake affected mainly in Palu Central City. Furthermore, 1.5 meters of tsunami occurred in Palu and Donggala coastal area. Additionally, massive liquefaction also occurred in some part of Palu Areas and caused severe damage in the affected areas.

Liquefaction is closely related to the geological and geomorphological characteristics as liquefaction often occurs again in the same location [20-22]. By using a similar approach, the liquefaction assessment was conducted in the study area. Furthermore, this study also analyses the liquefaction from the share-wave velocity and seismic vulnerability index point of view. By knowing the share-wave velocity and seismic index vulnerability, the potential site of liquefaction can be identified [12, 21]. The higher value of ground share-strain indicates the easier the ground deformation will occur, and it will lead to a crack, liquefaction, and event coseismic landslide [24]. The relationship of the shear-strain value and the potential liquefaction can be seen in Table 2 below.

Table 2 The shear-strain value and soil dynamic.

Size of strain	10^{-6}	10^{-5}	10^{-4}	10^{-3}	10^{-2}	10^{-1}
Phenomena	Wave, Vibration	Crack, Diff Settlement			Landslide, Compaction, liquefaction	Soil and
Dynamic Properties	Elasticity		Elasto Plasticity	Repeat-effect	Speed-effect of Loading	

Source: [24].

Based on this concept, the combination of probabilistic seismic hazard assessment (PSHA) and the Ishihara concept was used to analyse the potential liquefaction area in the study area. Thus, the first step of this analysis is to generate the peak ground acceleration (PGA) based on the historical earthquake data. Further, the PGA value was used to assess the ground shear strain based on the earthquake vulnerability index (Kg).

The complete workflow to assess the potential liquefaction area in the study area is provided in Figure 6 below.

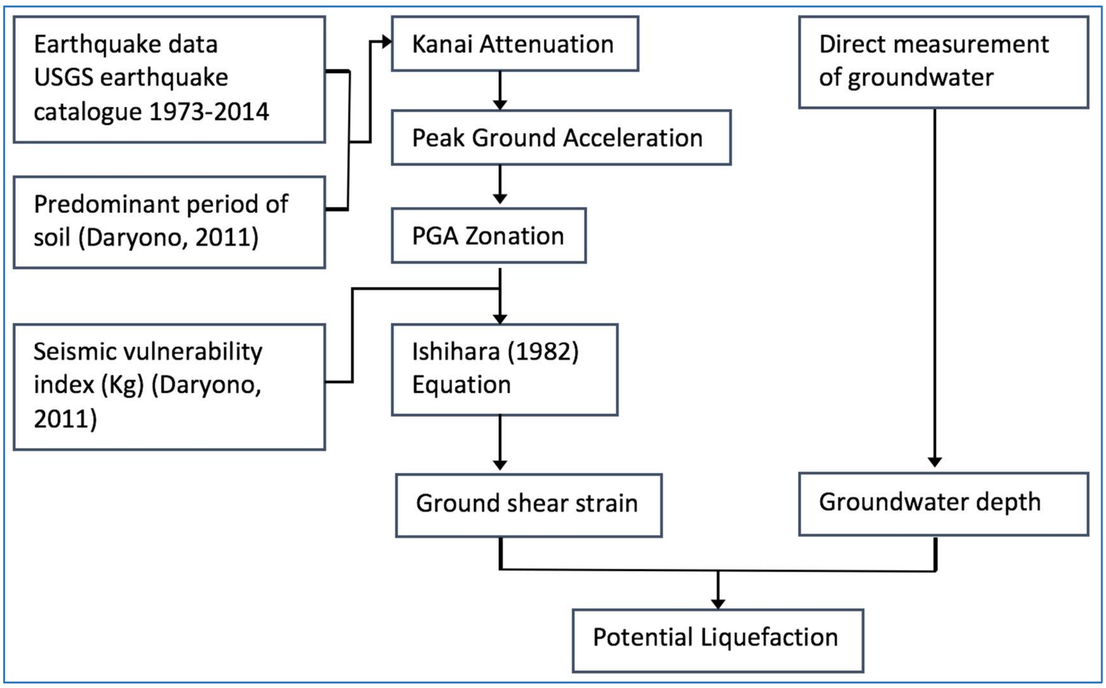

Fig. 6 The potential liquefaction assessment

3.6. The multi-vulnerability assessment

The multi-vulnerability assessment used in this study followed the previous research which was conducted by [15]. This research applied logistic regression analysis in order to predict the damage level of the residential building based on the Yogyakarta earthquake, 27 May 2006 damage data. The main data used in that research were earthquake damage data, Quickbird image, geologic map, and building footprint data. The earthquake damage data was obtained from [16], which consists of building damage data (low, medium, and collapsed) in impacted area (Jetis, Pleret, Imogiri, Bantul Sub-District). The Quikcbird imagery was used to obtain the land use data in more actual and detail scale (the year 2012, scale 1:25.000) based on the modified Anderson system 2002 [25]. [15] used the geology map of Yogyakarta to extract the additional data such as the lithology, type of material, and distance from the epicentre of Yogyakarta earthquake (27 May 2006).

In general, there were two main elements at risk used in the analysis such as population and building collapsed probability. The population data was obtained from the local statistics agency (BPS), meanwhile the building collapsed probability was generated from the logistic regression analysis. There are four steps of analysis to conduct the multi-vulnerability assessment. The first step was to extract the land use data by using visual interpretation of Quickbird imagery. The second step was to conduct the probability of building collapsed. The third step was to conduct the population distribution model and the last step was to combine the building collapsed probability and population distribution into multi-vulnerability analysis. The complete step of multi-vulnerability analysis is provided in Figure 7 below.

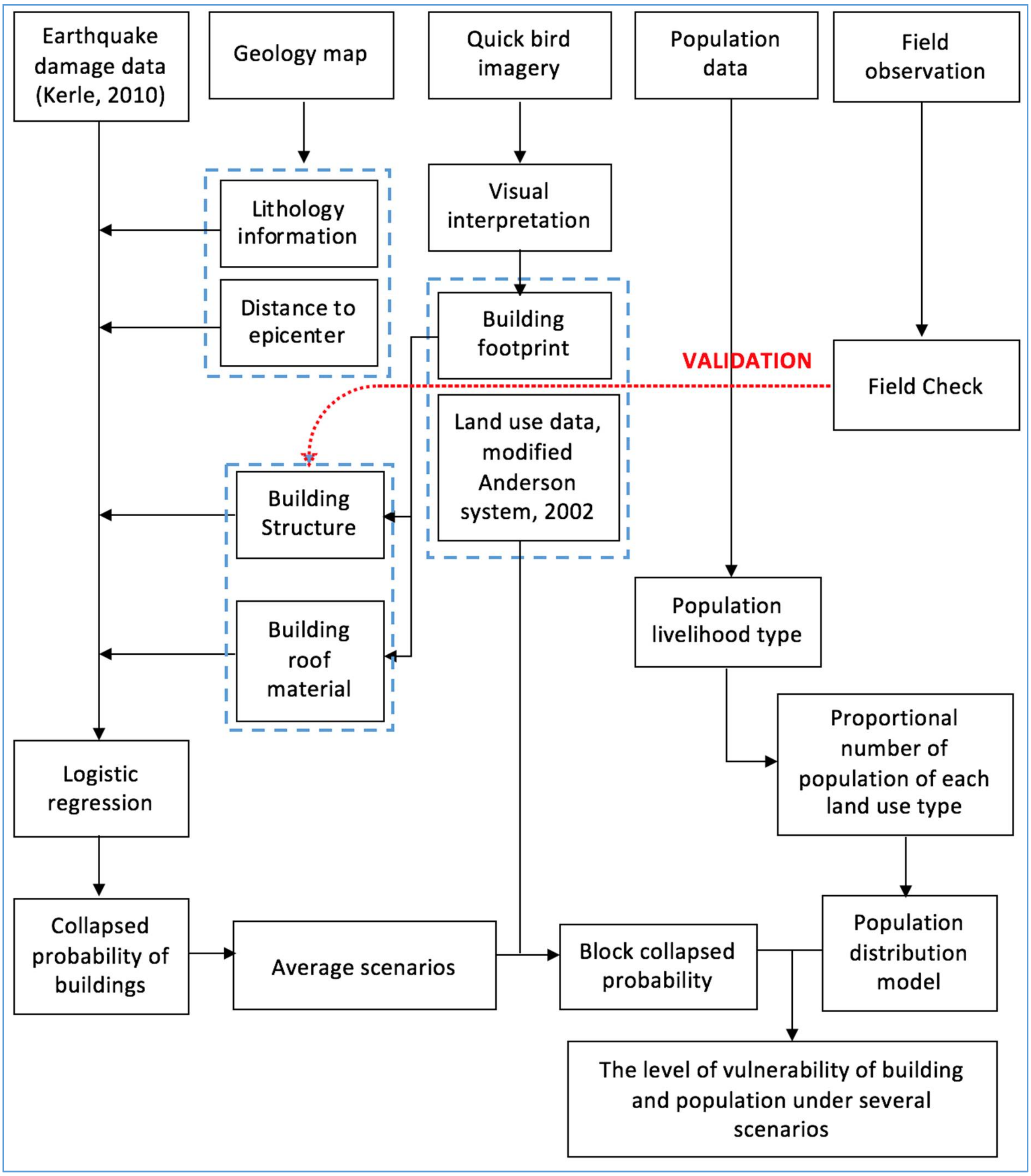

Fig. 7. The general workflow of multi-vulnerability analysis

3.7. Multi-hazard and risk assessment

The approach to generate the multi-hazard and risk assessment followed the general concept of risk assessment and reduction. The risk is the function of hazard and vulnerability. It can be expressed as follow:

$R = H.\mathrm{V}$ ....(1)

where R is the risk, H is hazard, and V is Vulnerability.

The multi-hazard and risk scheme of this study referred to the [26], which considered the hazards as the combination of ground motion, soil amplification, liquefaction, and coseismic landslide. Meanwhile, in term of vulnerability, this study was focused only in building block (building collapsed probability) and the population (the population distribution). The multi-hazard and risk assessment of earthquake and other related secondary hazards applied in this study is provided in the Figure 8 below.

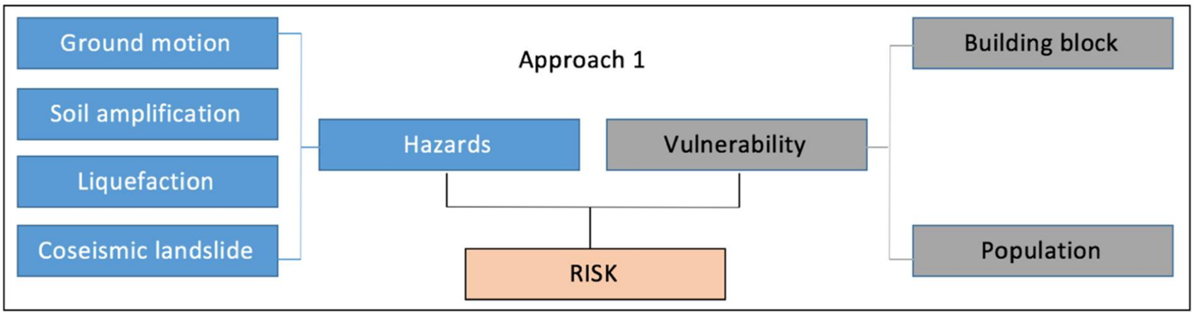

Fig. 8. The multi-hazards and risk assessment, source [26]

Thus, based on Figure 8 above, the general equation 1 was modified to accommodate the multihazard aspect in this study. Equation 2 shows how the multihazard and risk was generated in this study.

$$Multi\ Risk = Multihazard\ (P + SA + L + CL)\ .\ \mathrm{Multivulnerability\ (BV + PV)} \quad \ldots\ldots\ldots\ldots(2)$$

Where P is PGA value, SA is soil amplification, L is liquefaction, CL is a coseismic landslide, BV is building vulnerability, and PV is population vulnerability.

4. Results and discussion

4.1. Peak Ground Amplification

Based on the Kanai attenuation over 3,481 earthquakes historical data with the magnitude more than 5 Richter Scale which occurred between 1973 and 2014, the peak ground acceleration of study area ranges from 531.04 to 967.66 cm/s2. Theoretically, the higher PGA value in the particular area shows the higher degree of damage probability when the earthquake occurs [27-28]. Based on this attenuation, the higher PGA value is located also in the middle part of study area and extends to northeast and southeast direction along the Opak River which is closely associated with the location of Opak Fault. In other side, the lower PGA value spreads northwest part to Yogyakarta City direction. This distribution of PGA value has inverse relation with the dominant period of soil. Based on the direct measurement by using microtremor which was conducted by [12] explained that the highest (0.84) predominant period of soil in study area is located in the northwest part area. The predominant period of soil and PGA are provided in Figure 9A and B below.

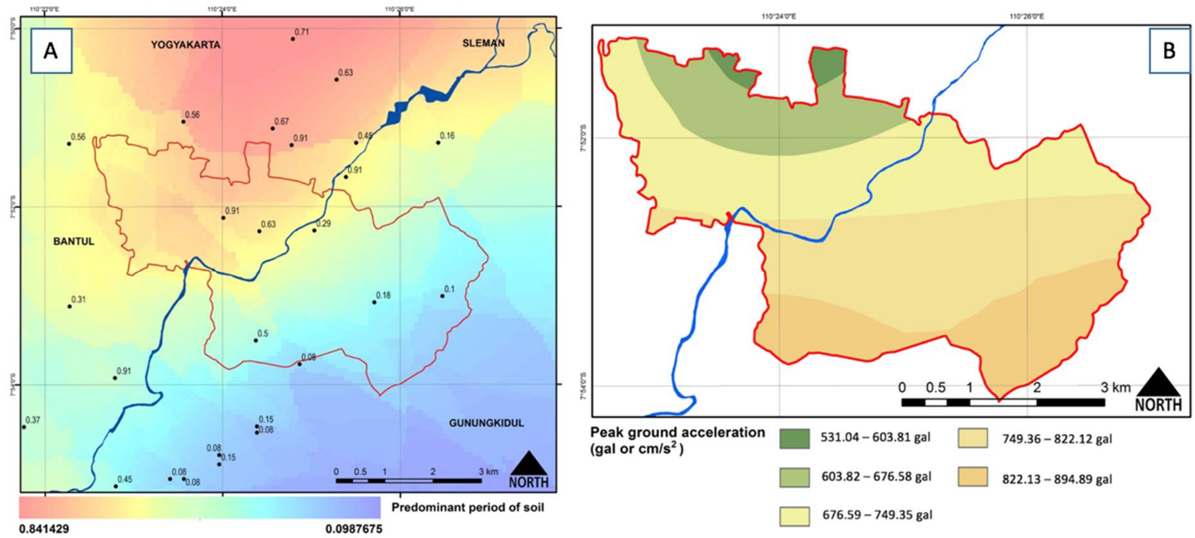

Fig. 9 A) The predominant period of soil in study area; B) Peak ground acceleration (PGA) in study area.

4.2. Results of Outcrop study.

Based on the outcrop study which was conducted by [8], the study area has a complex geological structure condition. This study also found the significant evidence of faults displacement including the great normal fault in this area namely Opak Fault. [8] found the same rock of Nglanggran Formation (The Tmn is described as a volcanic breccia, lava flow containing breccia agglomerate rock, and tuff). The main location of the Nglanggran formation is at the summit of Baturagung Escarpment. However, based on the field observation they found an isolated hill of Nglanggran Formation which located in the centre of study is, approximately 4.24 km separated from the main location of Nglanggran Formation. Additionally, [8] found that the middle parts of the study area are more vulnerable to ground amplification. At least, 30 faults displacement were found in the middle part of the study area with a maximum displacement of 2.39 m. Most of the faults are typically normal fault, and only a few of them are a strike-slip fault. Also, the direction most of the micro faults are similar to the direction of Opak Fault. The outcrop study conducted by [8] revealed that the Segoroyoso Village, Srumbung Sub Village, Middle part of Bawuran Village, Middle part of Pleret Village, and middle part of Wonolelo Village are vulnerable due to the complex geological structure and ground amplification. The map of fault evidence derived from outcrop study and the example of maximum faults displacement in Srumbung Sub-Village are provided in Figure 10 and 11, respectively.

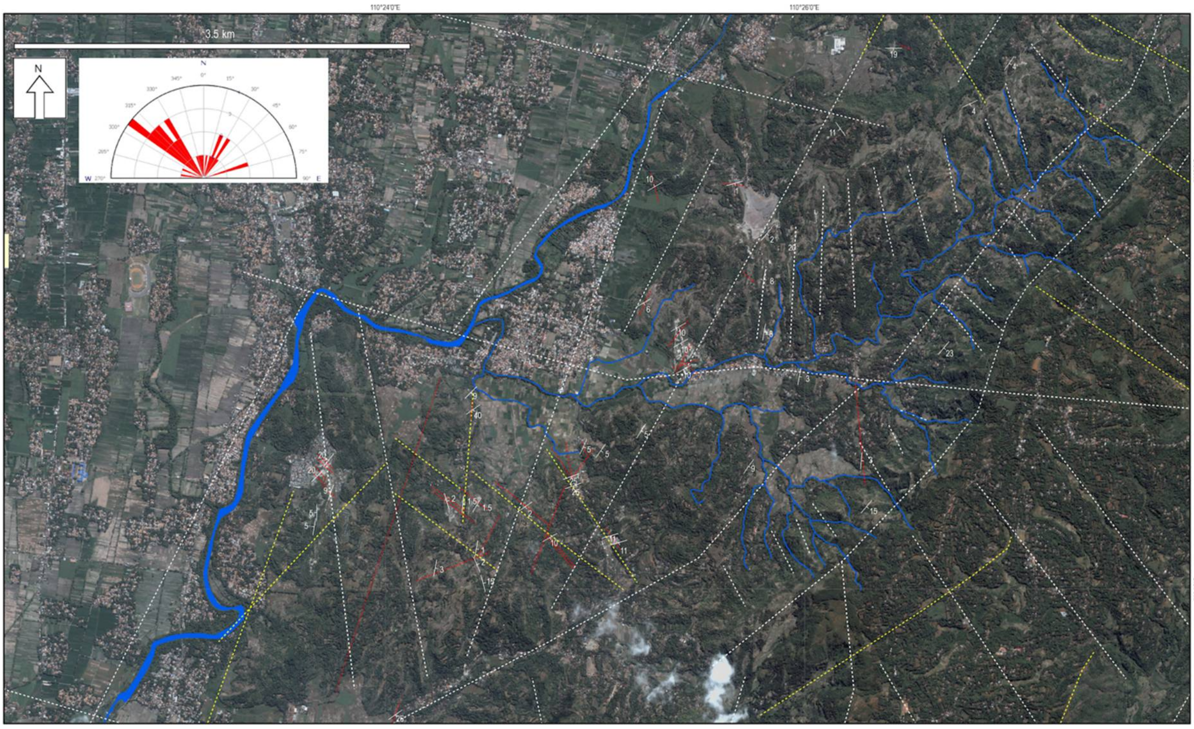

Fig. 10. Fault reconstruction and lineament in study area.

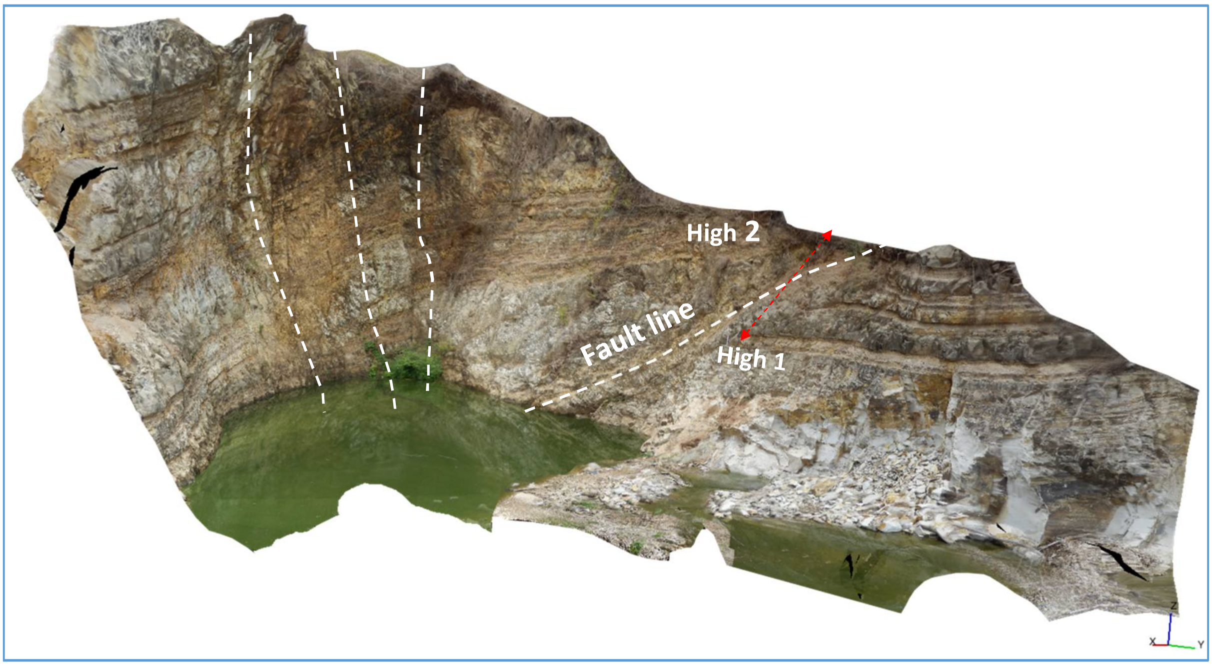

Fig. 11. Fault displacement in outcrop number 15, Srumbung Sub-Village.

4.3. Liquefaction results

4.3.1. The groundwater condition

Based on the integrated direct measurement of household wells during the 2015 rainy season, some geo-electricity observations especially in fluvial plain and local people drilling activities in South Segoroyoso, the study area are dominated by the shallow groundwater area (less than 10 m). This abundance groundwater area is concentrated in the middle part of the study area (Wonokromo, Pleret, middle Segoroyoso, Middle Bawuran, and Middle Wonolelo). Geomorphologically, this area is dominated by the fluvial plain and colluvial plain which consists of Alluvium from Young Merapi Volcanic Deposit (Qmi) and Colluvium from denudational material of Semilir and Nglangran mountainous area (Qa), respectively (Fig 12)

Inline with the household wells observation, the geo-electricity observation showed that the study area has abundance groundwater. The shallow groundwater can be found at a depth of 2.5-15 m in the colluvial plain in the narrow plain east part of the study area. Further, from the borehole data, we also got a similar variation of groundwater depth. In alluvial and colluvial plain the shallow groundwater can be found in the depth of 1-15 m. This shallow aquifer is known as a confined aquifer. Meanwhile, the deep aquifer can be found in the depth of approximately 80-110 m.

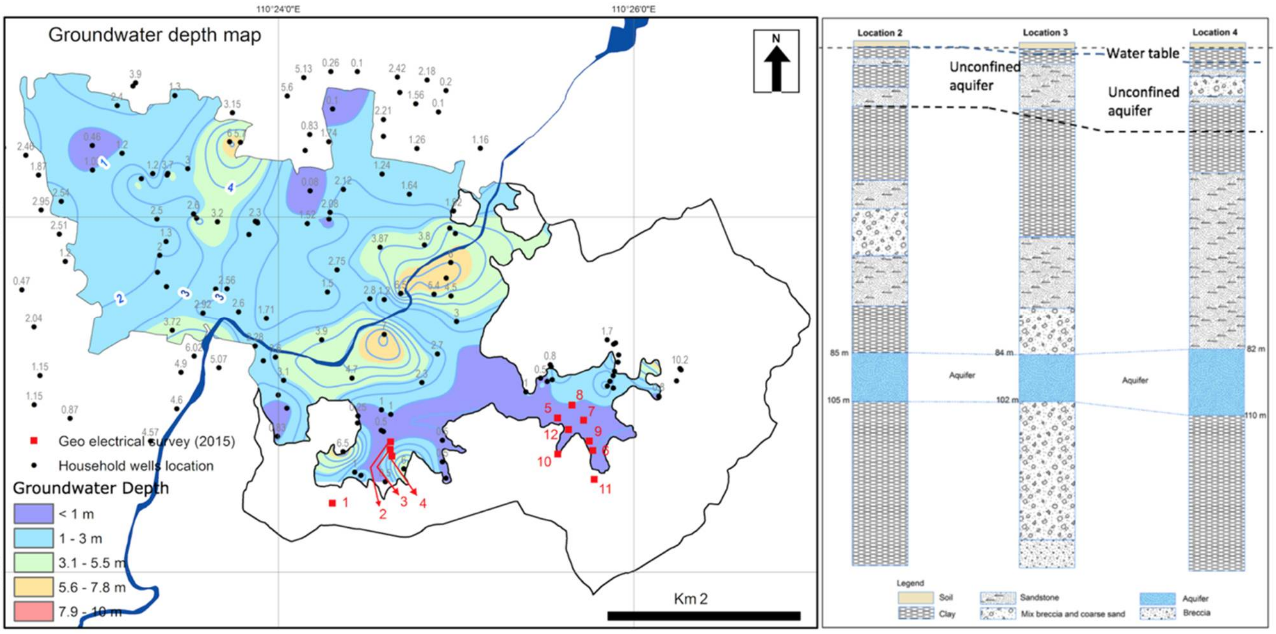

Fig, 12 The groundwater depth (Left); Groundwater characteristic of location 2, 3, and 4 based on the drilling data

4.3.2. The liquefaction

Based on the ground-shear strain and the potential liquefaction by using Ishihara method, the more prone areas to liquefaction are the middle part of study area especially in Kerto, Keputren, and Kanggotan Village (Fig. 13). This area has the highest ground-shear strain of 9,221.43 x 10^{-6} which

Preprints (www.preprints.org) | NOT PEER-REVIEWED | Posted: 18 December 2018 doi:10.20944/preprints201812.0213.v1

belongs to alluvial plain of young Merapi volcanic deposits with the sediment thickness of 130 m and groundwater depth around 2.31 m.

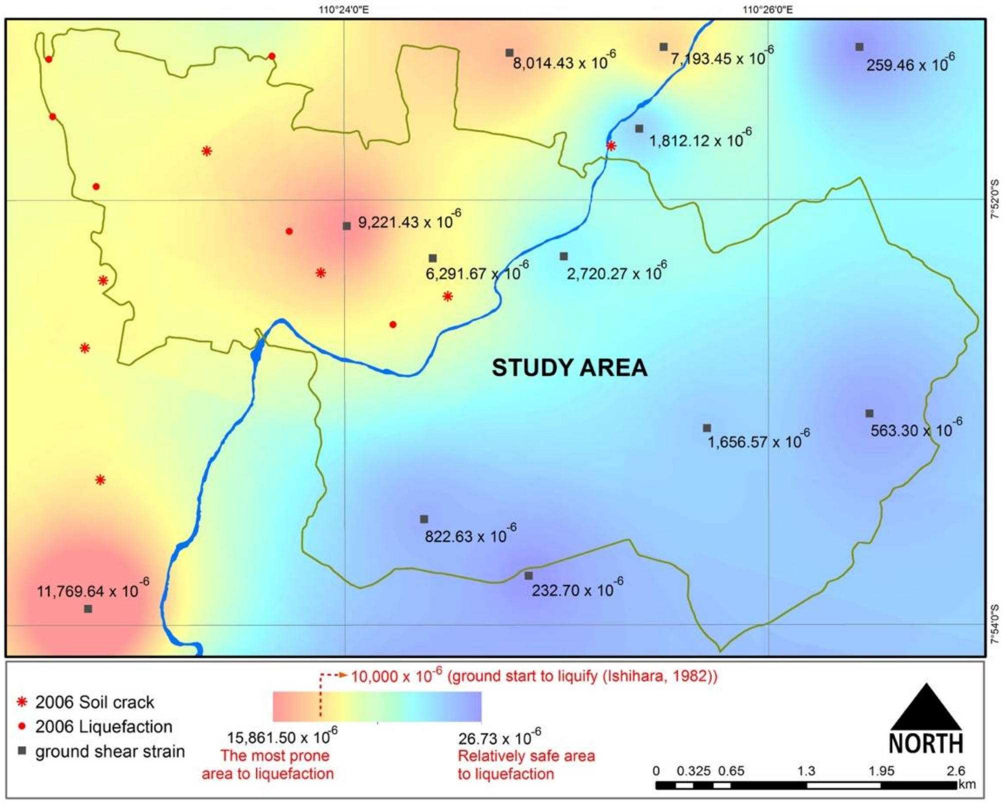

Fig. 13. Potential Liquefaction model in study area.

4.4. Coseismic landslide

Based on the [13-14], the study area could be classified into four Coseismic Landslide Susceptibility Level (CLSL) namely, negligible, low, moderate and medium CLSL. The negligible zone is the safest area in the study area. This zone mainly distributes in the west part to the middle part of the study area. This zone located in flat to gentle slope area and located in the alluvial plain zone, colluvial plain and natural levee of Opak River. The low zone associated with the narrow plain that located in the border area between the flat and mountainous area in the east part study area. The moderate zones are mainly located in the middle slope of Baturagung Escarpment which has characteristic of weak to strong eroded denudational hills of Semilir Formation. The medium zone or considered as the most unstable areas are located in upper slope of Baturagung Escarpment which consists of Semilir Formation. The complete figure of coseismic landslide susceptibility map can be seen in Figure 14 below.

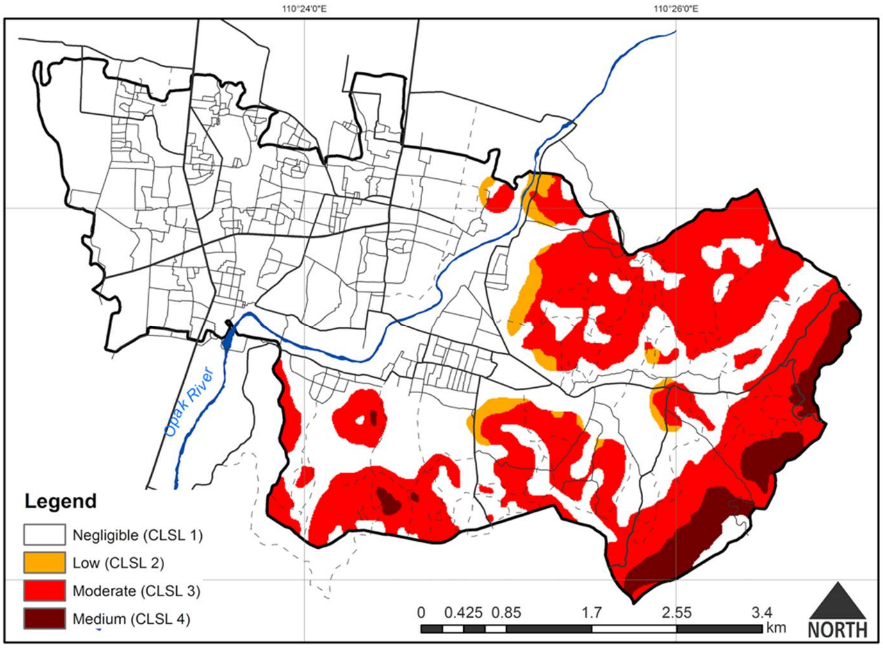

Fig. 14. The potential coseismic landslide susceptibility level (CLSL) in study area.

4.5. Multi-vulnerability results

The first element at risk used in this study was residential buildings. The vulnerability of residential buildings was generated from the logistic regression. There were two datasets used in this study. The first dataset was the building damage data due to the Yogyakarta earthquake data. This data consists of some information of attribute data such as location (x and y), the owner, the building structure, the roof material, geology, the distance from the epicentre and the level of damage. This data was obtained from field observation right after the disaster occurrence [14]. Meanwhile, the second dataset was the building footprint data of existing buildings after rehabilitation and reconstruction process. This data was generated from visual interpretation process. This data has the same attribute contains such as location (x and y), the type of buildings structure, roof materials, geology and the distance from the epicentre.

The other data element at risk was population density. This study used the dasymetric technique to generate the population density per unit land use. Several scenarios such as the population of each land use unit in daytime and night-time both in weekday and holiday were also applied to obtain the real population condition. The land use units were generated from the visual interpretation based on the Anderson classification. The vulnerability results of each element at risk will explain as follow. Meanwhile the results of multi-vulnerability are provided in Figure 20.

4.5.1. Land use based on visual interpretation of Quick bird imagery.

Based on the modified Anderson system 2002 [25] there were 29 land use units found in the study area. This land use unit covers the classification level III which suitable for interpretation of Quickbird or medium-altitude data taken between 10,000 and 40,000 feet (3,100 and 12,400 m) or 1: 20,000 to 1: 80,000 scale of the map. Based on this classification, the study area can be categorised into 29 land use units namely, Abandoned mining sites, agricultural wetlands, canal, cemetery, cemetery on wetland, commercial strip development, educational institution, government centres, harvested cropland, health institution, inactive cropland, light industrial, not built up, open areas, other agricultural, other institutional (mosque), pastureland, poultry farm, residential high density, residential low density, residential medium density, rural single unit, road, shrubland, specialty farm, stone quarries, stream, traditional market, and wetlands. The distribution and the total area of land use units are provided in Figure 15 below.

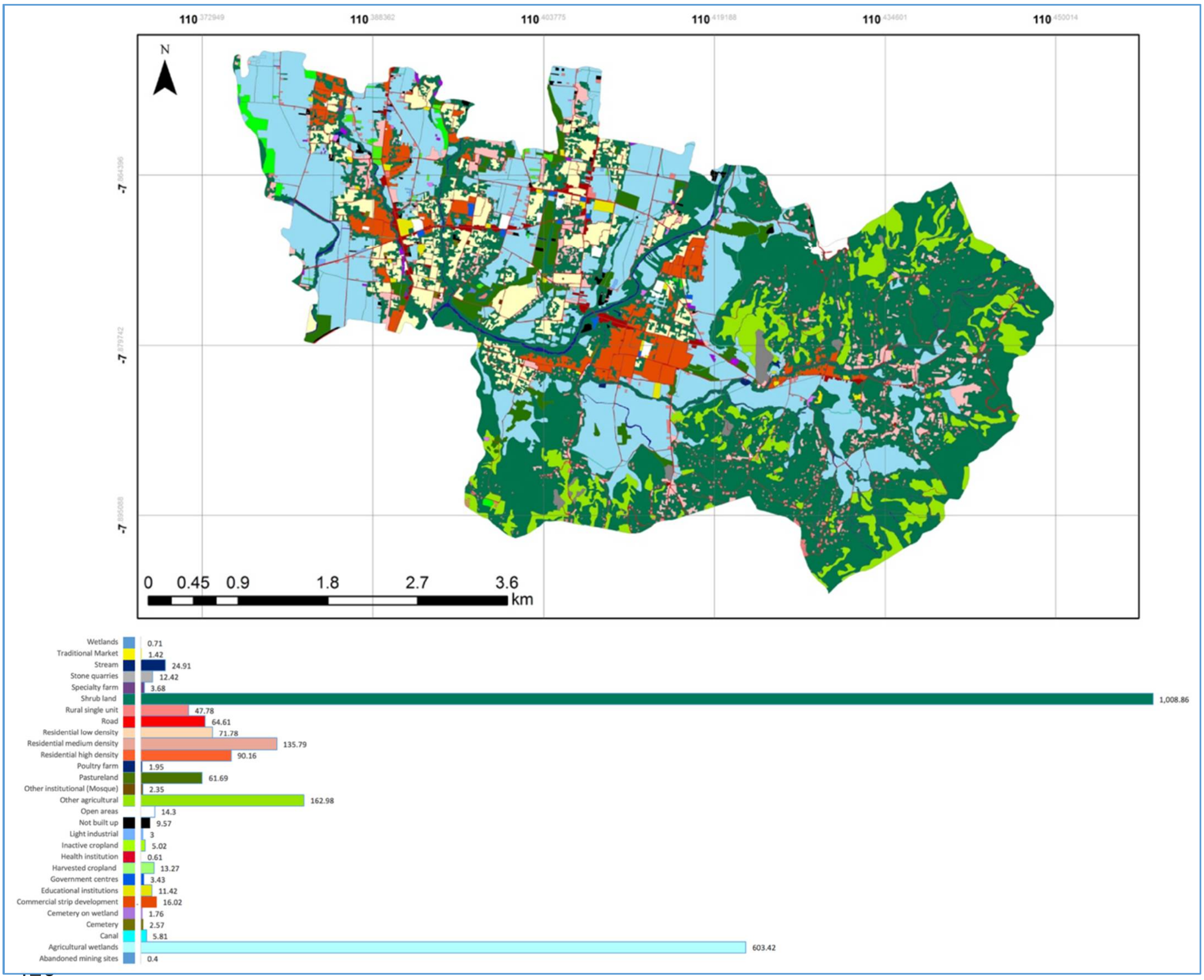

Fig. 15. The land use map and its total area.

4.5.2. Building unit collapsed probability

There were three main results based on the logistic regression; first, the results of model fitness, second, pseudo r-square, and the third, parameter estimates value. The model of fitness' shows that the model (binary coding) the parameters both independent and dependent variables were significant, fit and can be used for further analysis (Table 3). The pseudo r-square result provides information about how far the model can explain the results. Based on the logistic regression, the model can explain at least 33.20% which indicated from the Nagelkerke value (Table 4). This means there are 66.80% of dependent variable cannot be explained from this model. Thus, stated in the recommendation part that some parameters need to be added for the next research.

The parameter estimates value (Table 5) shows that the threshold values of the damage categories are 1.529 and 2.426 for the damage category 1 and 2 respectively. This means the predicted response value (Y*i) were categorised as follow:

- Damage category 1 (low damage) if Y*i ≤ 1.529
- Damage category 2 (moderate damage) if 1.529 < Y*i < 2.246
- Damage category 3 (Collapsed) if Y*i ≥ 2.246

The Y value can be estimated from the formula which was derived from the value of each parameter in Table 5. The formula followed general regression equation. Therefore, from Table 5 the general equation of damage probability is expressed as:

$$\boldsymbol{Y * i = -0.255\,(X1) + 0.685\,(X2) + 0\,(X3) + 0.43\,(X4) + 0.749\,(X5) + 1.634\,(X6) + 0\,(X7) + 2.265\,(X8) + 0.949\,(X\ \ ) + 0.744\,(X10) + 0\,(X11) - 1.413\,(X12) - 0.64\,(X13) + 1.507\,(X14) + 0\,(X15)} \text{..} \mathbf{1)}$$

Where the Y*i is the prediction value of damage probability; X1 is wood structure; X2 is unreinforced masonry; 0 reinforced masonry; X4 is asbestos and zinc; X5 is cement tile; X6 is Clay tile roof; X7 is concrete slap roof; X8 is distance within 8 km from epicentre; X9 is distance between 8.1 – 10 km; X10 is distance between 10.1 – 15 km; X11 is distance above 15 km; X12 is Semilir formation (Tmse); X13 is alluvium (Qa); X14 is young volcanic deposits of Merapi Volcano (Qmi), and X15 is Nglanggran Formation (Tmn).

Based on the visual interpretation of 17,512 buildings, there were only 33 combinations of house characteristics. Each combination has specific building attributes and damage category. For instance, the combination number 5, wood structure, clay tile roof, distance more than 15 km from the 2006 epicentre, and young volcanic deposit of Merapi Volcano, has the value of Y*I of 2.886 which means belongs to damage category 3 or collapsed. The illustration of how to assess the damage category prediction in the study area can be seen in Figure 16 below.

Example of how to entry the binary code of each variable

ID	St0	St1	St2	Rf0	Rf1	Rf2	Rf3	Dst1	Dst2	Dst3	Dst4	Geo0	Geo1	Geo2	Geo3
1	0	0	1	0	0	1	0	0	1	0	0	0	0	1	0
2	0	0	1	0	0	1	0	0	1	0	0	0	0	1	0
3	0	0	1	1	0	0	0	1	0	0	0	0	0	1	0
4	0	1	0	0	0	1	0	0	1	0	0	0	0	1	0
↓															
21	0	1	0	0	0	1	0	0	1	0	0	0	1	0	0

Damage categories calculation

ID	St0	St1	St2	Rf0	Rf1	Rf2	Rf3	Dst1	Dst2	Dst3	Dst4	Geo0	Geo1	Geo2	Geo3
1	0	0	.43	0	0	1.63	0	0	.95	0	0	0	0	-.64	0
2	0	0	.43	0	0	1.63	0	0	.95	0	0	0	0	-.64	0
3	0	0	.43	.43	0	0	0	2.26	0	0	0	0	0	-.64	0
4	0	.68	0	0	0	1.63	0	0	.95	0	0	0	0	-.64	0
↓															
21	0	.68	0	0	0	1.63	0	0	.95	0	0	0	-1.41	0	0

Example of damage categories
ID 1 → DC = 0.43 + 1.63 + 0.95 – 0.64 = 2.37, which belong to DC2 or moderate damage
ID 3 → DC = 0.43 + 0.43 + 2.26 – 0.64 = 2.48, which belong to DC 3 or collapsed
Etc.

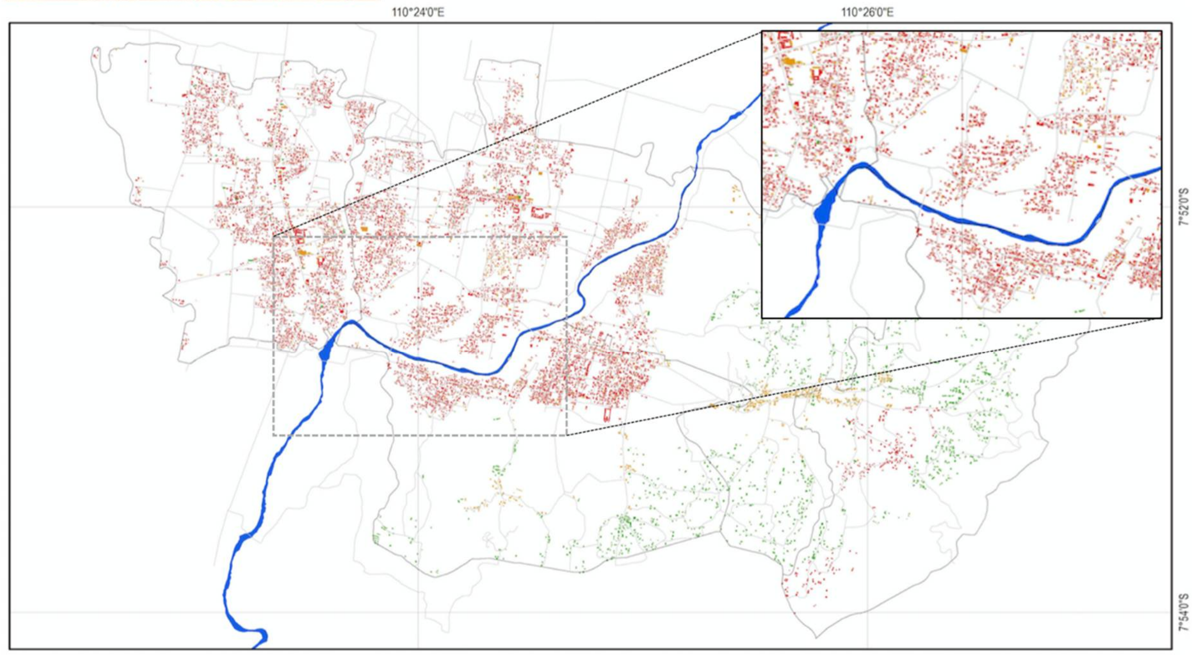

Figure 16. Illustration of how to classify the buildings existence into several damage categories.

The building probability of collapsed can be calculated by following formula:

$$Probability\ of\ no\ damage\ (Y1) = \frac{1}{1+e^{(Y*i-threshold\ 1)}} \ldots\ldots 2)$$

$$Probability\ of\ moderate\ damage\ (Y2) = \frac{1}{1+e^{(Y*i-threshold\ 2)}} - \mathrm{Y1} \ldots\ldots 3)$$

$$Probability\ of\ no\ damage\ (Y3) = 1 - \frac{1}{1+e^{(Y*i-threshold\ 2)}} \ldots\ldots 4)$$

Thus, for example, The combination number 5 (wood structure, clay tile roof, distance more than 15 km from the 2006 epicentre, and young volcanic deposit of Merapi Volcano) was categorized to damage category 3 or collapsed. By using equation 4 above how big the probability of collapse can be generated. For instance, the combination number 5 has the value of Y*1 2.886. Therefore, the probability of collapsed was,

$$Y3 = 1 - \frac{1}{1+2.718^{(2.886-2.426)}}$$

$$Y3 = 1 - \frac{1}{1+e^{(0.46)}}$$

$$Y3 = 1 - \frac{1}{1+1.58}$$

$$Y3 = 1 - \frac{1}{2.58}$$

$$Y3 = 1 - 0.387$$

$$Y3 = 0.613.$$

Based on the calculation above, the building combination number 5 (wood structure, clay tile roof, distance more than 15 km from the 2006 epicentre, and young volcanic deposit of Merapi Volcano) has predicted damage category of 3 (collapsed) with the probability of 0.613. Further, by applying equation 2, 3, and 4 to the existing building footprint, the probability of collapsed of each combination can be known. The safest building type in the study area is the building with the attributes building combination of reinforced masonry structure, asbestos or zinc roof material, located between 10.1-12 km from the earthquake source, and located above the Semilir Formation with the probability of damage only 0.07. Meanwhile, the most vulnerable building is the building with the building attributes combination of reinforced masonry structure, clay tile roof material, located between 8.1 and 10 km, and located above the young volcanic deposits of Merapi Volcano. The probability of collapse of this type reaches 0.84.

Building block probability of collapsed was obtained from converting the probability of collapse of building unit into the block or land use scale. The average value was applied to convert the probability of collapse in building the unit to block unit. The illustration of how to convert the value and the result of building block collapsed probability are provided in Figure 17. Based on the results, the residential block which is located in the western part of the Opak Fault is dominated by the moderate vulnerability or probability of collapsed between 0.6 – 0.73. The middle part of a study area, in the left and right of Opak Riverbank, is dominated by the highest value of building collapsed probability. The value reaches 0.74 – 0.84 of collapsed probability. Meanwhile, the eastern part tends to have low collapsed probability (< 0.59), because this area is mountainous areas which consist of compact lithological characteristics.

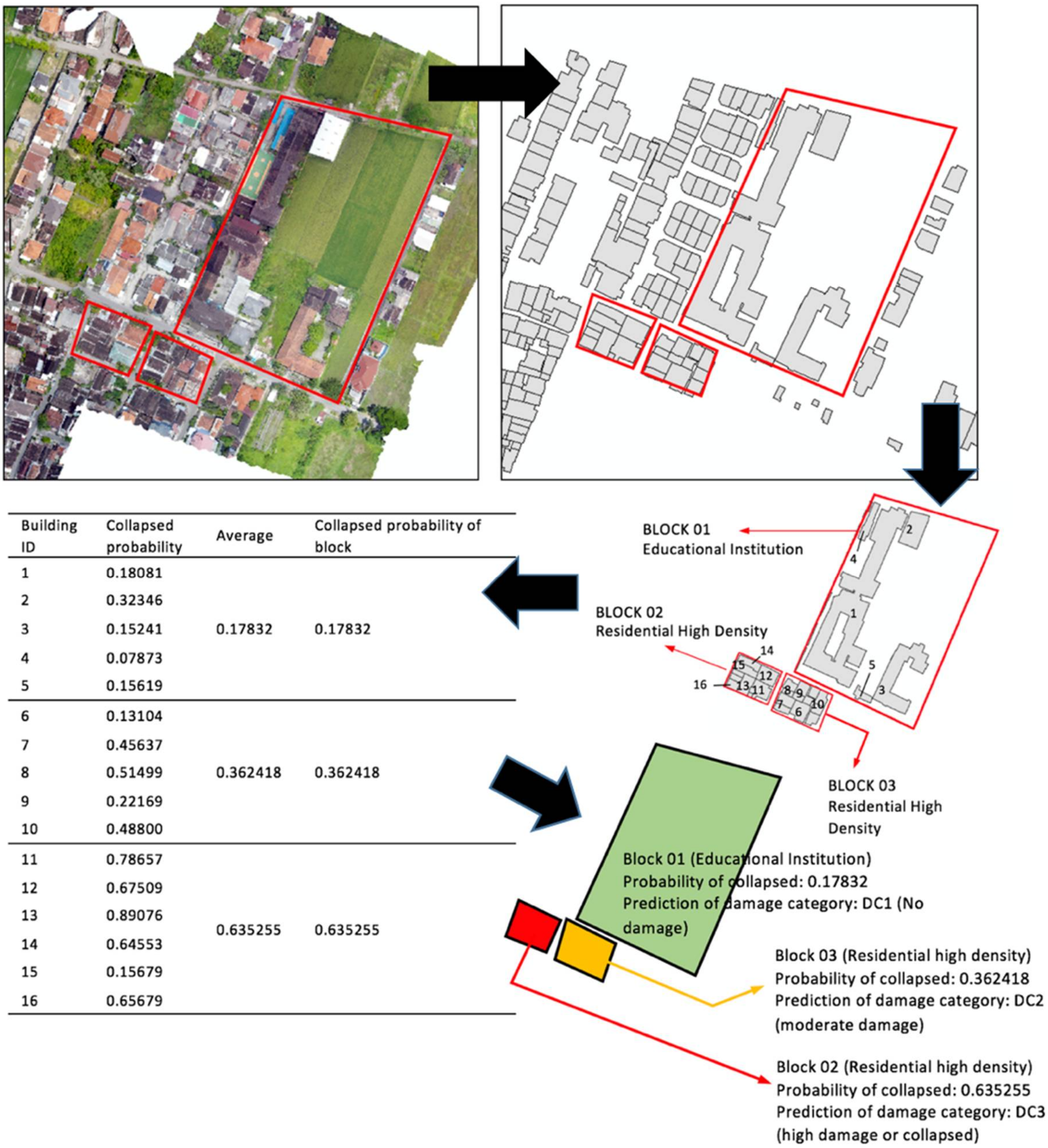

Building ID	Collapsed probability	Average	Collapsed probability of block
1	0.18081		
2	0.32346		
3	0.15241	0.17832	0.17832
4	0.07873		
5	0.15619		
6	0.13104		
7	0.45637		
8	0.51499	0.362418	0.362418
9	0.22169		
10	0.48800		
11	0.78657		
12	0.67509		
13	0.89076		
14	0.64553	0.635255	0.635255
15	0.15679		
16	0.65679		

Figure 17. The example of converting the building unit collapsed probability to block unit.

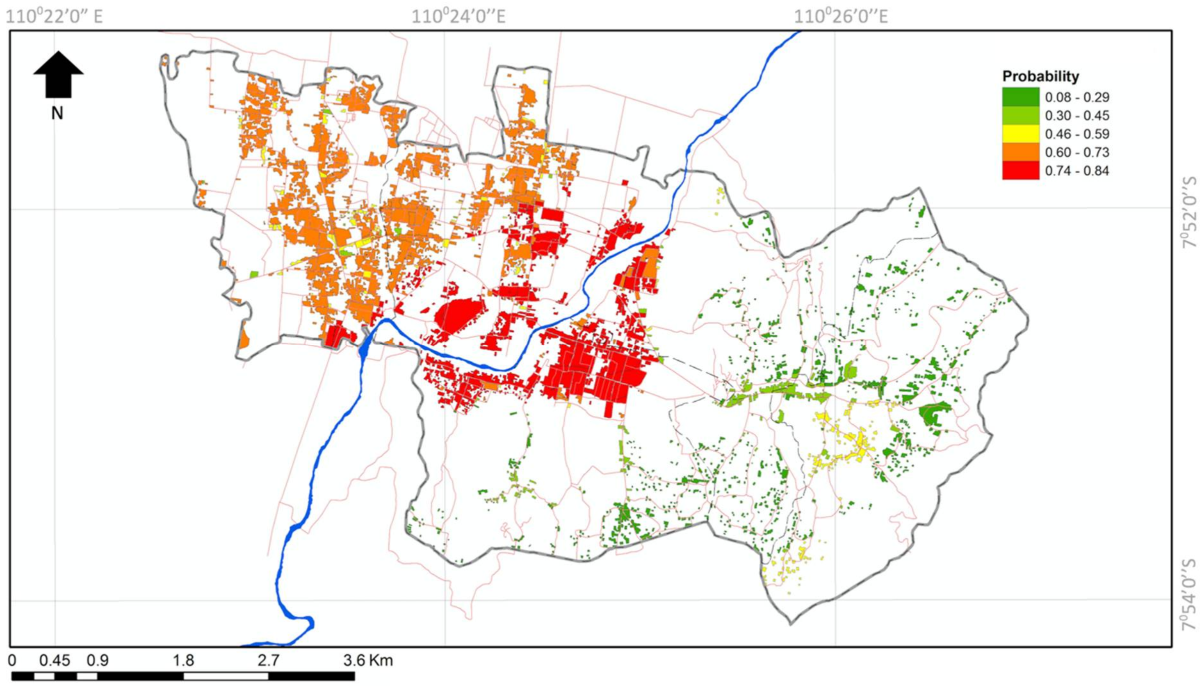

Figure 18. The collapsed probability of building block in study area

4.5.3. Population distribution model

The distribution of population on several scenarios (daytime-night time both on holiday and weekday), was defined based on the dasymetric analysis through the simple percentage of the occupation of the local people. Based on the data, people of Pleret Sub-District is dominated by the casual worker, student, unemployment, entrepreneur, and farmer who reaches 17.92%, 20.51%, 18.86%, 20.16%, and 23.99%, respectively. Thus, based on the dasymetric the population distribution on each block of land use can be estimated. For instance, during the work hour, the population in Wonokromo Villages, the densest village in the study area, tends to distribute into three major land use units such as settlement, school, and commercial areas. The number of population can be estimated at 27.7% stay in commercial areas, 16.65% in schools, and 16.47% in settlement areas. The rest amount of population distributes into other land use units. Similar to this condition, the population in other villages such as Pleret, Segoroyoso, Bawuran, and Wonolelo Villages mainly distribute into commercial areas, school, settlements, and agriculture areas. Furthermore, the population distribution in all villages in the study areas has no significant difference among the scenarios used. The population distribution under several scenarios are provided in Figure 19-20

Preprints (www.preprints.org) | NOT PEER-REVIEWED | Posted: 18 December 2018 doi:10.20944/preprints201812.0213.v1

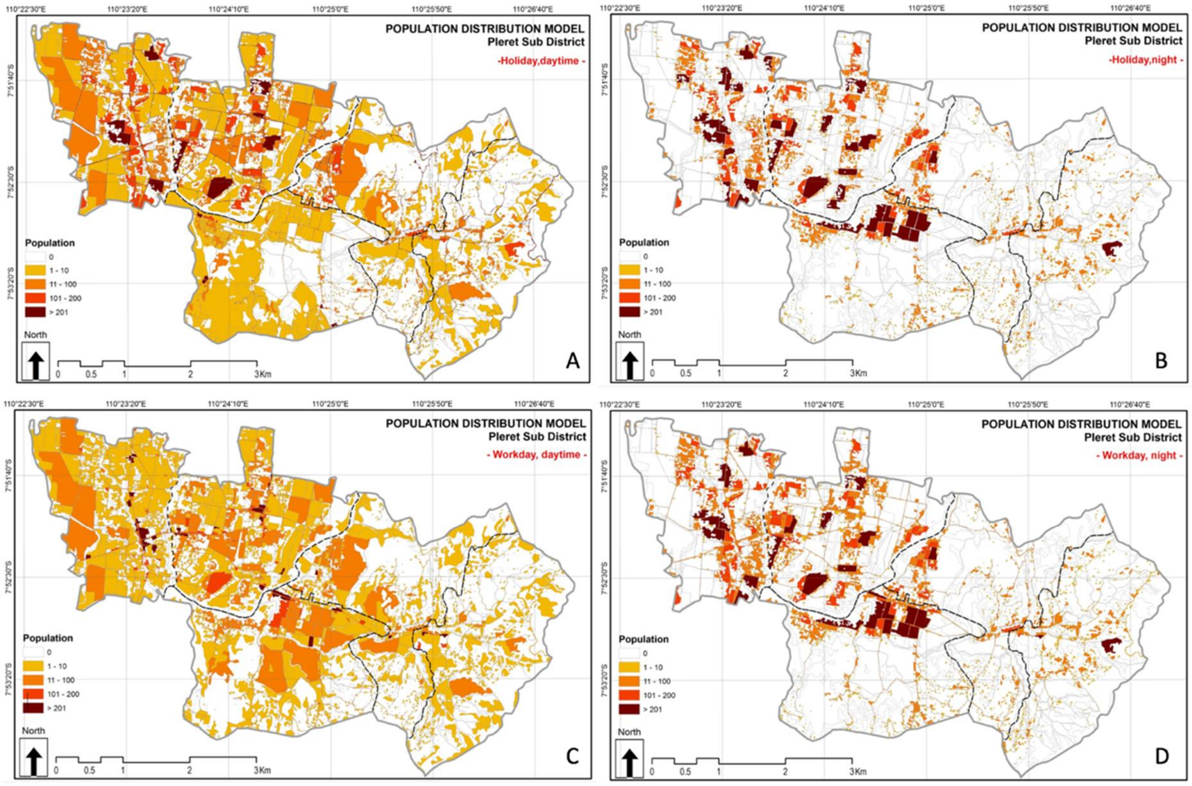

Figure 19. Population distribution; A) during holiday daytime, B) holiday nigh time, C) Work day daytime, and D) Work day nighttime

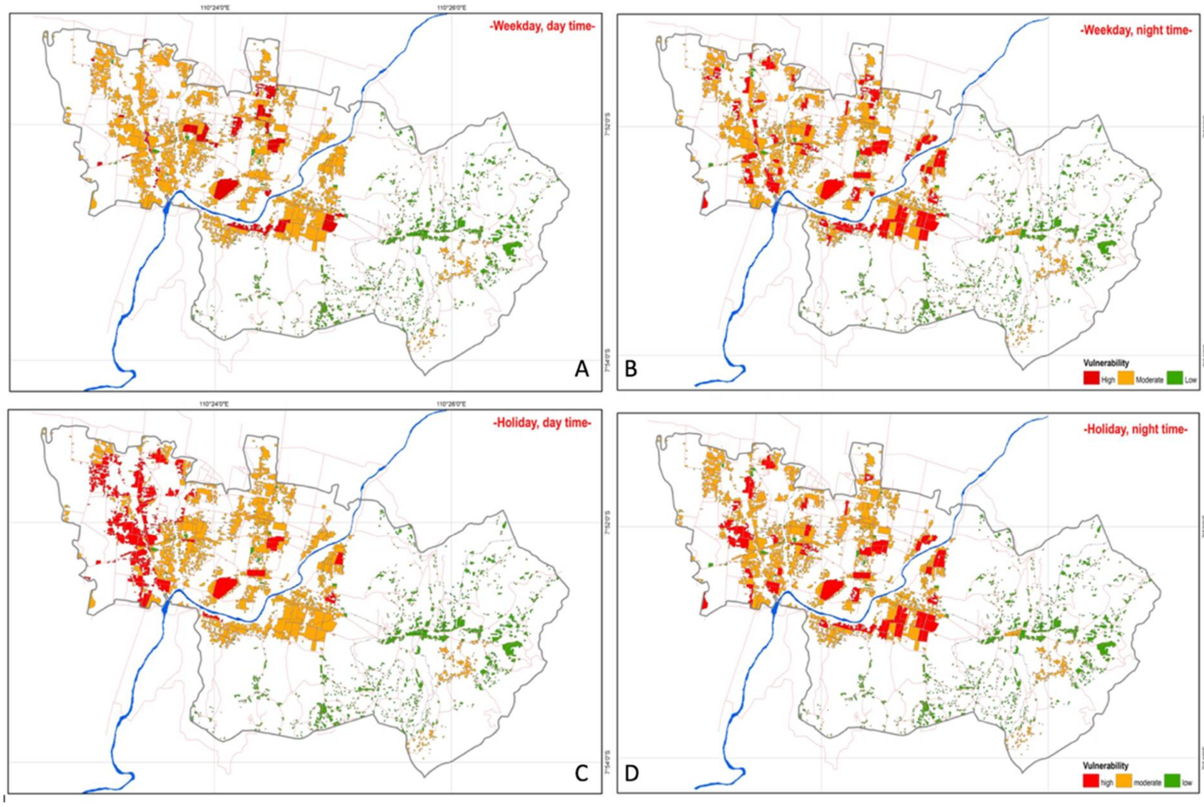

Figure 20. Multi-vulnerability; A) during holiday daytime, B) holiday nigh time, C) Work day daytime, and D) Work day nigh time

 doi:10.20944/preprints201812.0213.v1

4.6. Multi-Risk results

The multi-hazard zonation was generated by applying the summation function of all hazards parameters (PGA, the proximity of the faults, liquefaction, and coseismic landslide). The summation function was determined based on the consideration of the used hazards are secondary earthquake hazards which can amplify the earthquake impact. Based on the analysis, it can be known that the index of multi-hazard in the study area is between 0.46-0.85 with the minimum and maximum value of 0 and 1. Based on this analysis, the study area is dominated by the multi-hazard zone 0.61 which can be classified as the moderate multi-hazards zone. Most of this zone is located in the flat are in the middle part of the study area. These areas are located near to Opak Fault, have a complex geological structure, and has soft surface sediment of alluvium or colluvium. In term or PGA, this zone has PGA around 676.59-822.12 gal and low ground shear strain which means very vulnerable to ground motion and liquefaction occurrence. The total area of this zone reaches 39.12% of the study area (Figure 21).

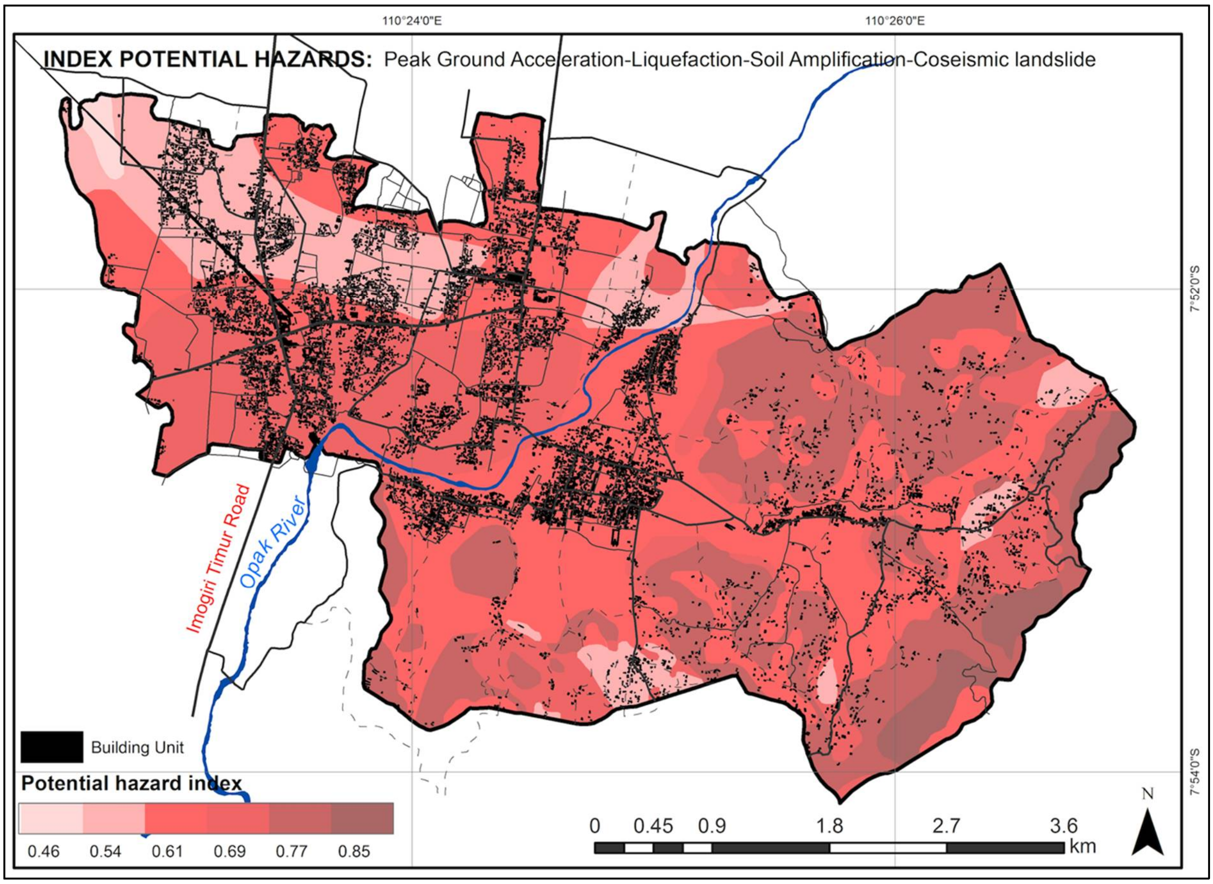

Hazards information: PGA was derived based on Kanai attenuation by using USGS earthquake historical data (1973-2014); Liquefaction was generated based on the ground shear strain value of USGS earthquake historical data (1973-2014); Soil amplification was assessed based on the proximity to active faults which was generated from outcrop study; Coseismic landslide was resulted from the coseismic landslide model grade 2 proposed by Mora and Vahrson (1999); and the multi-hazard index was generated from raster overlay function with benefits standardisation method.

Figure 21. Multi-hazards zonation in study area.

Preprints (www.preprints.org) | NOT PEER-REVIEWED | Posted: 18 December 2018 doi:10.20944/preprints201812.0213.v1

The multi-risk value can be obtained by adding the multi-temporal information of population distribution. The results show that both in daytime or night time of weekday, the middle part has high multi-risk value, because this area has higher value of multi-hazard index; high population density; and most of the buildings inside the block has higher probability of collapsed. Meanwhile, the holidays scenarios also give different results. Based on the holiday scenarios both daytime and night time the population tend to distribute in the residential block. For example, Segoroyoso Village slightly increased the multi-hazard risk assessment in the nigh time. The complete picture of multi-risk value is provided in Figure 22 below.

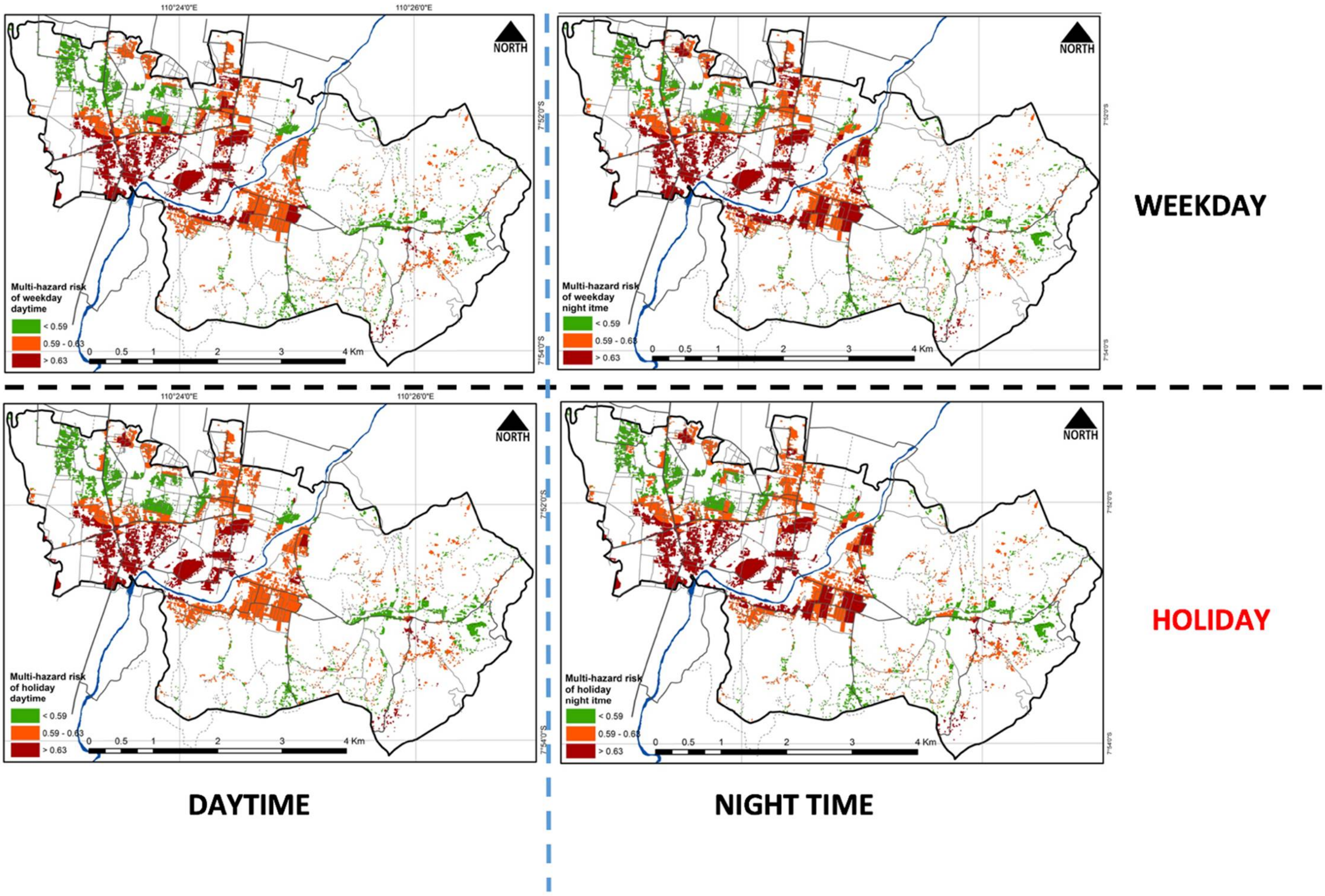

Figure 22. Multi-risk value in study area.

The multi-risk models give slightly different results between weekday and holiday multi-risk index and give very distinctive results of daytime and night time. On daytime both in weekday and holiday, the high multi-risk index mainly distributed in the south part of Wonokromo Village, in the middle part of Pleret Village, and some area of Wonolelo Villages. Meanwhile, in the nigh time both in weekday and holiday, the high multi-risk index is mainly distributed in most of the residential area in the study areas, as almost all people stay in the residential area during the night both in holiday and weekday. This model shows (Fig. 22 left picture) that the south part of Wonokromo Village, the middle part of Pleret Village, the middle part of Bawuran, Segoroyoso, and Wonolelo Villages, indicate the high multi-risk index.

Conclusion and recommendation

Based on the results above the multi-risk index of study area toward earthquake and other secondary hazards differs influenced by the PGA, ground motion, liquefaction, coseismic landslide, population distribution and building collapsed probability. Based on the CLSL analysis the study area consists of the negligible, low, moderate, and medium zone. The negligible and low CLSL are mainly distributed in the extensive flat area in the west part of the study area. Meanwhile, the more vulnerable area of CLSL is mainly distributed in the mountainous area in the middle part of the study area. Furthermore, this study also signifies that the middle slope of Baturagung Escarpment more prone to coseismic landslide occurrence. This finding is in line with the landslide study which was conducted in the western part of Yogyakarta [29].

Furthermore, this study also reveals that the study area has a complicated geological structure. Based on the lineament analysis, various lineaments feature of valleys, ridges, river, sudden changed of river direction, ridges line, scarp face, and straight drainage segment were founded. All these lineaments are associated with the existence of faults [30-31]. Based in the earthquake fracture displacement recorded on the outcrop surface, it is known that the middle part of the study area, around north to a middle part of Segeroyoso, middle part of Pleret and Bawuran, has a complex faults configuration which could be indicated from the dense area of faults and highest displacement. Additionally, based on the lithostratigraphic analysis it is known that the outcrop deposits were ignimbrite type, which was originated from the ancient volcano (tertiary) in the east part of study area.

Based on the shear strain analysis which was derived from the PGA analysis, the study area especially the extensive flat area in from middle to west parts are dominated with the area of shallow groundwater or up to 10 m depth and have a high value of ground shear-strain. This means this area is very vulnerable to liquefaction occurrence.

In term of vulnerability analysis, this study concluded that statistically, the building with the type of reinforced masonry structure (RM), clay tile roof material, was built above Young Volcanic Deposits of Merapi Volcano (Qmi) and 8.1 – 10 km located from the epicentre of 2006 earthquake, has a higher probability of collapsed. Meanwhile, in term of population distribution, there is no significant difference in population density on each land use unit between holiday and weekday. However, this study found that the population density on each land use unit has different between daytime and nighttime. Thus, it also affects the multi-risk index which has a different pattern in daytime and night time.

The multi-hazard risk results show that the residential houses which are located in the centre part of study area including the centre of Wonkromo, Pleret, Bawuran, and Wonolelo, also north part of Segoroyoso Villages have high multi-hazard and risk index (> 0.60) both in daytime and nighttime during the weekday and holiday. This means this area is more prone to earthquake hazards and other related secondary hazards.

Further, a good inventory data of landslide and coseismic landslide are needed to improve the coseismic landslide hazard result. Additionally, several site-specific observations also need to be done to support the coseismic landslide. Some limitation of liquefaction analysis was also found in this study such as this study was still used Ishihara model to approach the liquefaction. We need to conduct some standard penetration test (SPT) and cone penetration test (CPT) for verification. Lastly, the statistic analysis of building collapsed vulnerability needs to be improved by adding more parameters as independent variables such as soil type, the shape of buildings and], and the age of buildings.

Acknowledgement

This paper is part of the PhD research at Dept. of Geography, University of Canterbury, New Zealand, which is funded by the Indonesia Endowment Fund for Education (LPDP-Indonesia). The author is thankful to main supervisor, Dr. Christopher Gomez, who has supported this project, co supervisor Dr. Ioannis Delikostidis, Dr. Peyma Zawar-Reza, Dr. Danang Sri Hadmoko and Prof. Dr. Junun Sartohadi. We also acknowledge the University of Canterbury New Zealand who provided adequate reference for this project.

Authors' contribution

AS and CG collected the data, AS carried out the analysis, CG and ID support on the interpretation of the results. AS drafted the manuscript, CG, DSH, JS, ID, and PZ revised the manuscript. All the authors drafted, read and approved the final manuscript.

Competing interests

The authors declare that they have no competing interests.

References

1. Budimir, M.E.A.; Atkinson, P.M.; Lewis, H.G. Earthquake and landslide events are associated with more fatalities than earthquake alone. *Nat Hazards* **2014**, *72*, 895-914, doi: 10.1007/s11069-014-1044-4
2. van Westen, C. Risk analysis. *In Multi hazard risk assessment, distance education course, guide book*; van Westen, C., Alkema, D., Damen, M.C.J., Kerle, N., Kingma, N.C., Eds.; United Nations University-ITC School on Disaster Geo-Information Management (UNU-ITC DGIM): Twente, Netherland, 2011.
3. Ren, Z.L.; Liu, W. Typical disaster chains and cascading effect caused by 2012 Xinyuan Ms 6.6 earthquake and Ms 8.0 earthquake of China. In Proceedings of Sixth China-Japan-US Trilateral Symposium on Lifeline Earthquake Engineering, Chengdu, China, 28 May-1 June 2013; pp. 66-72.
4. Brook, K. Christchurch experience more flooding. Available online: https://www.canterbury.ac.nz/news/2014/christchurch-experiences-more-flooding.html (Accessed on 20 August 2017).
5. Irsyam, M.; Sengara, I.W.; Aldiamar, F.; Widiyantoro, S.; Triyoso, W.; Natawidjaja, D.H.; Kertapati, E.; Meilano, I.; Suhardjono; Asrurifak, M.; Ridwan, M. Ringkasan hasil studi tim revisi peta gempa Indonesia. Available online: http://www.preventionweb.net/files/14654_AIFDR.pdf. (Accessed on 25 January 2012).
6. Tim Pusat Studi Gempa Nasional. *Peta sumber dan bahaya gempa Indonesia tahun 2017*; Irsyam, M., Widiyantoro, S., Natawidjaja, D.H., Meilano, I., Rudyanto, A., Hidayati, S., Triyoso, W., Hanifa, N.R., Djarwadi D., Faizal, L., Sunarjito, Eds.; Pusat Penelitian dan Pengembangan Perumahan dan Permukiman, Badan Penelitian dan Pengembangan, Kementrian Pekerjaan Umum dan Perumahan Rakyat: Bandung, Indonesia, 2017; Volume 1, ISBN 978-602-5489-01-3.
7. Nurwihastuti, D.W.; Sartohadi, J.; Mardiatno, J.; Nehren, U.; Restu. Understanding of earthquake damage pattern through geomorphological approach: A case study of 2006 earthquake in Bantul, Yogyakarta, Indonesia. *World J. Eng. Technol.* **2014,** *2*, 61-70, doi: 10.4236/wjet.2014.23B010.
8. Saputra, A.; Gomez, C.; Delikostidis, I.; Zawar-Reza, P.; Hadmoko, D.S.; Sartohadi, J.; Setiawan, M.A. Determining earthquake susceptible areas southeast of Yogyakarta, Indonesia-Outcrop analysis from structure from motion (SfM) and geographic information system (GIS). *Geosciences* **2018,** *8*, 132, doi: 10.3390/geosciences804132.
9. Bronto, S.; Mulyaningsih, S.; Hartono, G.; Astuti, B. Gunungapi purba Watuadeg: Sumber erupsi dan posisi stratigrafi. *Jurnal Geologi Indonesia* **2008,** *3 (3),* 117-128.
10. Winarti; Hartono, G.H. Identification of volcanic rocks in Imogiri Yogyakarta based on subsurface geologic data. In Proceedings of 2nd International Conference on Engineering of Tarumanegara (ICET), Jakarta, Indonesia, 22-23 October 2015.
11. Pandita, H.; Sukartono; Isjudarto, A. Geological identification of seismic source at Opak Fault based on stratigraphic section of the Southern Mountains. *Forum Geogr.* **2016,** *30 (1),* 77-85.
12. Daryono. Indeks kerentanan seismic berdasarkan mikrotremor pada setiap satuan bentuklahan di zona graben Bantul Daerah Istimewa Yogyakarta. Doctoral Thesis, Universitas Gadjah Mada, Yogyakarta, Indonesia; 2011.
13. Saputra, A.; Sartohadi, J.; Hadmoko, D.S.; and Gomez, C. Geospatial assessment of coseismic landslide in Baturagung Area. *Forum Geogr.* **2015,** *29 (2),* 99-114.
14. Saputra, A.; Gomez, C.; Hadmoko, D.S.; Sartohadi, J. Coseismic landslide susceptibility assessment using geographic information system. *Geoenviron. Disaster* **2016**, *3*, 27, doi: 10.1186/s40677-016-0059-4
15. Saputra, A.; Rahardianto, T.; Revinda, M.D.; Delikostidis, I.; Hadmoko, D.S.; Sartohadi, J.; Gomez, C. Seismic vulnerability assessment of residential buildings using logistic regression and geographic information system (Yogyakarta-Indonesia). *Geoenviron. Disaster* **2017**, *4*, doi: 10.1186/s40677-017-0075-z.
16. Kerle, N. Satellite-based damage mapping following the 2006 Indonesia Earthquake-How accurate was it? *Int. J Appl. Earth Obs. Geoinf*. **2010,** 12, 466-476, doi: 10.1016/j.jag.2010.07.004.

17. Mora, S.; Vahrson, W. Microzonation for slope instability in Costa Rica. *In Manual for zonation on seismic geotechnical hazards (Revised version)*; Technical Committee for Earthquake Geotechnical Engineering, TC4, ISSMGE., Ed.; The Japanese Geotechnical Society: Tokyo, Japan, 1999.
18. Chu, D.B.; Stewart, J.P.; Lee, S.; Tsai, J.S.; Lin, P.S.; Chu, B.L.; Seed, R.B.; Hsu, S.C.; Yu, M.S.; Wang, M.C.H. Documentation of soil conditions at liquefaction and non-liquefaction sites from 1999 Chi-Chi (Taiwan) earthquake. *Soil. Dyn. Earthquake Eng*. **2004,** *24* (9-10), 647-657, doi: 10.1016/j.soildyn.2004.06.005.
19. Morgenroth, J.; Hughes, M.W.; Curbinovski, M. Object-based image analysis for mapping earthquake-induced liquefaction ejecta in Christchurch, New Zealand. *Nat Hazards* **2016,** *82*, 763-775, doi: 10.1007/s11069-016-2217-0
20. Youd, T.L.; Perkins, D.M. Mapping of liquefaction severity index. *J. Geotech. Engrg*. **1987**, *113* (11), 1374-1392.
21. Yasuda, S.; Tohno, I. Sites of Reliquefaction Caused by the Nihonkai-Chubu Earthquake. *Soils Found* **1988**, *28*(2), 61-72.
22. Tatsuoka, F.; lwasaki, T.; Tokida, K.; Yasuda, S.; Hirose, M.; lmai, T.; Kon-no, M. Standard penetration tests and soil liquefaction potential evaluation. *Soils Found* **1980**, *20* (4), 95-111, doi: 10.3208/sandf1972.20.4_95.
23. Huang, H.; Tseng, Y. Characteristics of soil liquefaction using H/V of microtremor in Yuan-Lin area, Taiwan. *TAO* **2002**,*13* (3), 325-338.
24. Ishihara, K. Evaluation of Soil Properties for Use in Earthquake Response Analysis, In Geomechanical Modelling in Engineering Prectice; Dungar, R., Studer, J.A., Eds.; Balkema: Rotterdam, Netherland, 1982.
25. U.S. Geological Survey. Land use cover classification system NJDEP modified Anderson system. Available online: http://www.state.nj.us/dep/gis/digidownload/metadata/lulc02/anderson2002.html (Accessed 6 September 2016).
26. Alkema, D.; Boerboom, L.G.J.; Ferlisi, S.; Cascini, L. Caribbean handbook on risk information management ACE-EU. Available online: http://www.charim.net/print/93. (Accessed 13 January 2018).
27. Yamazaki, F; Matsuoka, M. Remote Sensing Tools for Earthquake Response and Recovery. In proceedings of International Symposium on Remote Sensing Applications to Natural Hazard, Beijing, China, 12-17 October 2008.
28. Walter, T. R.; et al. The 26 May 2006 magnitude 6.4 Yogyakarta earthquake south of Mt. Merapi volcano: Did lahar deposits amplify ground shaking and thus lead to the disaster? *Geochem. Geophys. Geosyst* **2008**, *9*, doi:10.1029 /2007GC001810, 2008.
29. Samodra, G., Chen, G.; Sartohadi, J.; Hadmoko, D.S.; Kasama, K.; Setiawan, M.A. Rockfall susceptibility zoning based on back analysis of rockfall deposits inventory in Gunung Kelir, Java. *Landslides* **2016**, *13*, 805, doi: 10.1007/s10346-016-0713-7.
30. Gannouni, S.; Gabtni, H. Structural interpretation of lineaments by satellite image processing (Landsat TM) in the region of Zahret Medien (Northern Tunisia). *Journal of Geographic Information System* **2015**, *7*, 119-127, doi: 10.4236/jgis.2015.72011
31. Lloyd, J. W. *Water resources of hard rock aquifers in arid and semi-arid zones.* United Nations Educational, Scientific and Cultural Organization (UNESCO): Paris, France, 1999.